

***Greb1* is required for axial elongation and segmentation
in vertebrate embryos.**

Ravindra Singh Prajapati^{1,2}, Richard Mitter³, Annalisa Vezzano^{1,4} and David
Ish-Horowicz^{5,6*}

¹Cancer Research UK Developmental Genetics Laboratory

²Present address: Centre for Craniofacial Development and Regenerative
Biology, King's College London, London, SE1 9RT, UK

³Francis Crick Institute, 1 Midland Rd, London NW1 1AT, UK

⁴Veyrier, 1255, Switzerland. vezzaro.annalisa@gmail.com

⁵Cancer Research UK Developmental Genetics Laboratory, and University
College London.

^{6*}Communicating author. Present address: Medical Research Council
Laboratory of Molecular Biology, University College London, Gower St,
London WC1E 6BT

*Correspondence: d.ish-horowicz@ucl.ac.uk

Keywords: tailbud, neural tube, axial stem cells, somites. transcriptome;
progenitors; clock

ABSTRACT

During vertebrate embryonic development, the formation of axial structures is driven by a population of stem-like cells that reside in a region of the tailbud called the chordoneural hinge (CNH). We have compared the mouse CNH transcriptome with those of surrounding tissues and shown that the CNH and tailbud mesoderm are transcriptionally similar, and distinct from the presomitic mesoderm. Amongst CNH-enriched genes are several that are required for axial elongation, including *Wnt3a*, *Cdx2*, *Brachyury/T* and *Fgf8*, and androgen/estrogen receptor nuclear signalling components such as *Greb1*. We show that the pattern and duration of tailbud *Greb1* expression is conserved in mouse, zebrafish, and chicken embryos, and that *Greb1* is required for axial elongation and somitogenesis in zebrafish embryos. The axial truncation phenotype of *Greb1* morphant embryos can be explained by much reduced expression of *No tail (Ntl/Brachyury)* which is required for axial progenitor maintenance. Posterior segmentation defects in the morphants (including misexpression of genes such as *mespb*, *myoD* and *papC*) appear to result, in part, from lost expression of the segmentation clock gene, *her7*.

INTRODUCTION

Vertebrate embryos develop in a highly organized fashion, progressively laying down axial tissues as they elongate along the anteroposterior embryonic axis (Brown and Storey, 2000; Catala et al., 1996; Wilson and Beddington, 1996; Wilson et al., 2009). Serial transplantation and other lineage tracing studies in mouse and chick have shown that a self-maintaining region in the tailbud called the chordoneural hinge (CNH) includes multipotent stem-cell-like progenitors for axial structures (Brown and Storey, 2000; Catala et al., 1996; Wilson and Beddington, 1996; Wilson et al., 2009). These include bipotent neuromesodermal progenitors (NMPs) that can generate both neural and mesodermal cells (Cambray and Wilson, 2002; Cambray and Wilson, 2007; McGrew et al., 2008; Selleck and Stern, 1991; Tam and Tan, 1992; Tzouanacou et al., 2009).

Adjacent to the CNH is the tailbud mesoderm (TBM) which contains the unsegmented precursors of the paraxial mesoderm, the presomitic mesoderm (PSM; Fig. 1A). During elongation, the PSM is displaced posteriorly while its anterior buds off a series of somites, epithelial balls that develop into segmental mesodermal structures such as the axial skeleton and musculature (reviewed in Pourquie, 2011)

Several studies have illuminated how axial progenitors are maintained during anteroposterior elongation. Briefly, a positive feedback loop between *Brachyury/T* and *Wnt3a* maintains axial progenitors in the tail bud (Martin and Kimelman, 2010; Wilson et al., 2009). In parallel, *Fgf* signalling protects axial progenitors from differentiation induced by Retinoic acid (RA) that is secreted by differentiating and young somites and diffuses into the PSM (Diez del Corral et al., 2003; Olivera-Martinez et al., 2012; Ribes et al., 2009).

However, *Fgf8*, *Wnt3*, and *T* are all expressed in much larger domains than the CNH and so do not specifically distinguish axial progenitors from more specialised cells such as the TBM. Transcriptome analysis of dissected axial

progenitor tissue during the period of axial elongation and of in vitro-derived NMPs has identified genes that are differentially expressed between progenitors and presomitic mesoderm cells (Gouti et al., 2017; Olivera-Martinez et al., 2014; Wymeersch et al., 2019). However, the functional significance of many of these genes has yet to be defined.

In this paper, we explore the transcriptional profiles of the CNH, TBM and PSM of E10.5 mouse embryos. We find that the CNH transcriptome is very similar to that of the TBM, and significantly different from that of the PSM. Several genes are expressed in both the CNH and TBM but not in the PSM, although none exclusively mark the CNH. Amongst the CNH-enriched transcripts is *Greb1* which encodes a transcriptional co-activator for androgen/estrogen hormone signalling. We show that *Greb1* is expressed in the tailbud in mouse, chick and zebrafish embryos, and is required for axial progenitor maintenance and somite compartmentalisation in zebrafish. Our results indicate that *Greb1* plays an evolutionarily-conserved role during vertebrate axial extension and segmentation.

RESULTS AND DISCUSSION

CNH transcriptome is distinct from PSM but not TBM

To identify potential markers for the CNH, we used microarray analysis on dissected tissue regions to identify genes whose expression in the E10.5 mouse CNH is elevated relative to that in the PSM and TBM (Fig. 1A). Hierarchical clustering of the replicate transcriptome patterns confirmed that the transcriptional profiles of the CNH, PSM and TBM are distinct (Fig.1B; Materials and Methods). Differential gene expression analyses identified 150 upregulated and 98 downregulated genes comparing the CNH to the PSM. The most significantly changed genes are listed briefly in Tables 1, and the complete in Supplementary Table S1. Only 12 up- and 2 down-regulated transcripts distinguished the CNH and TBM, consistent with the latter population being directly derived from the former (Tables 1, S1).

To confirm that many genes identified by microarray analysis are selectively expressed in progenitor regions of the extending embryo, we searched the Mouse Genome Informatics (MGI) database (Finger et al., 2017) for the expression patterns of 53 genes whose expression were upregulated ≥ 2 -fold in the CNH (Fig. 1C). A majority of these genes (29/53) are annotated as being expressed in tissues related to axial elongation, i.e., in one or more of the primitive streak, node, tailbud, and future spinal cord (Tables 2, S2). By contrast, most downregulated genes (23/27 reduced ≥ 2 -fold) are expressed in more specialised progeny cells, i.e., somites, unsegmented mesoderm or neural tube (Tables 2, S2).

Greb1 expression coincides with axial elongation in vertebrate embryos

We also compared our list of CNH-enriched genes with those previously identified in previous studies of the CNH or NMPs (Table S3; Gouti et al., 2017; Olivera-Martinez et al., 2014; Wymeersch et al., 2019). Expression of seven of the ten most-enriched genes (*Fgf8*, *Cdx2*, *T*, *Wnt3a*, *Sp5*, *Evx1*, and *Fgf17*) was

previously reported in the CNH and TBM, and to be functionally important for axial development (Cambray and Wilson, 2007; Dunty et al., 2014; Maruoka et al., 1998; Takada et al., 1994).

The expression and roles of the two most CNH-enriched genes from our study [*Defcr-rs7*, *Defcr-rs6* (which encode small immune-defect peptides) during axial elongation and segmentation remains to be studied. *Greb1*, which encodes a co-activator of the Estrogen and Androgen receptors that is active in human estrogen-receptor-positive primary breast and prostate cancer cells (Lee et al., 2019; Mohammed et al., 2013), is another top CNH enriched gene. Indeed, androgen receptor nuclear signalling is the most CNH-enriched pathway revealed by pathway enrichment analysis of our differentially expressed genes (Fig. 1D; Table S4; Supplementary Information). Other androgen-responsive genes also enriched in the CNH include *P21*, *cyclinD1*, and *MMP2* (Table S3). Indeed, the *MMP2* matrix metalloproteinase is required for axial elongation; morpholino knockdown of *MMP2* in zebrafish embryos, results in severe axial truncations (Zhang et al, 2003). Further studies will be required to test if androgen signalling operates in axial patterning.

Expression of chick *Greb1* in the axial stem cells zone has been described previously (Olivera-Martinez et al., 2014). We expanded this finding by examining *Greb1* expression during segmentation, using three different vertebrate systems. First, we visualised *Greb1* transcription in elongating mouse embryos using *in situ* hybridisation (E10.5-E13.5; Materials and Methods). In early (E8.5) embryos, *Greb1* is expressed in a posterior domain that encompasses the caudal lateral epiblast, the region that includes the axial progenitors (Fig. 2A,A'). By E10.5, labelling is restricted to the CNH and dorsal TBM (Fig. 2B,B'). Expression in these regions is maintained during axial elongation, albeit more weakly by E12.5, and is lost at E13.5 when axial elongation ceases (Fig. 2C,D).

The above results show that, although not restricted to the CNH, axial *Greb1* transcription in early mouse embryos coincides in time and place with the processes of axial extension and segmentation. To test if this correlation is evolutionarily conserved, we examined *Greb1* expression in chick and zebrafish embryos. In both animals, *Greb1* expression in the tailbud starts during elongation, and terminates when elongation and segmentation is complete. *Greb1* is expressed in the HH13 chick caudal neural plate, whose cells contribute to the neural tube, somites, and notochord, node and primitive streak (Fig. 2E,E'). Its axial transcription then becomes confined to the region of the tailbud which includes the chick CNH and TBM (HH17; Fig. 2F; McGrew et al., 2008), and has almost completely decayed when elongation is complete (HH26; Fig. 2G).

In zebrafish embryos, *Greb1* transcription becomes confined to the region of the tailbud that contains axial progenitors (Fig. 2H-L). It persists during segmentation (11-16 hpf; Fig. 2I-K), and disappears when axial elongation comes to an end (24 hpf; Fig. 2L). This conserved spatial and temporal time course in early vertebrate embryos strengthens the link between *Greb1* expression and axial extension.

Knock-down of *GREB1* disrupts axial elongation

To test if *Greb1* is functionally required during elongation and segmentation, we knocked down its expression by injecting antisense morpholinos into 1-2 cell zebrafish embryos (Materials and Methods). We used two *Greb1* splicing-blocking morpholinos (M1 and M2) that target the exon2-intron2 and exon16-intron16 boundaries, respectively (Fig. S1). These oligos should interfere with mRNA splicing to cause skipping of the adjacent exon and a shifted translational reading frame. The ensuing premature translational termination would completely truncate *Greb1* protein (M1) or encode one that is only 40% full-length (M2). As a control, we also injected a mismatched morpholino (MM) based on M2 but with 5 bases mutated to prevent binding to the primary *Greb1* transcript.

We verified the splice-blocking activities of both morpholinos via RT-PCR on RNA from injected embryos. *Greb1* splice variants corresponding to misprocessed transcripts were detected in M1- and M2-injected morphants but not MM morphant embryos (Fig. S1). DNA sequencing of these variant products confirmed that they result from skipping of the appropriate exons: exon 2 for oligo M1, and exon16 for M2 (Fig. S1).

We assayed the effects of *Greb1* knockdown 24 h after injection into embryos, when extension and segmentation is complete. M1 and M2 morphant embryos suffer three major axial defects: a curved trunk; a reduction in total body length (head-to-tail); misshaped somites and indistinct somite boundaries predominantly in more posterior axial regions (Fig. 3A-C). Injection of 4 ng/ μ l blocking oligonucleotide generates a high frequency of embryos showing all three defects (50/107 injected embryos for M1; 61/110 embryos for M2). No such abnormalities are seen in embryos injected with the control MM morpholino (0/15). Injecting 2 ng/ μ l of morpholino causes similar defects, albeit at lower frequencies (M1: 11/46; M2: 15/36; MM: 0/8).

These phenotypes are not due to unspecific toxicity from the injection. We co-injected each morpholino with one that knocks down *p53* expression, thereby preventing previously reported oligo-induced *p53*-dependent cell death (Supplementary Methods; Robu et al., 2007). Each blocking morpholino still efficiently caused axial extension and segmentation phenotypes (M1: 20/30; M2: 25/37; control MM: 0/10). Together, our data suggest that normal axial elongation and segmentation are dependent on *Greb1* activity.

***Greb1* is needed to maintain *Ntl* expression in the tailbud**

The axial truncations of *Greb1* morphants resembles the phenotype of embryos mutant for *No tail (Ntl)*, the zebrafish homologue of *Brachyury/T*, which is expressed in the tailbud, posterior PSM and notochord of wildtype embryos (Halpern et al., 1993; Schulte-Merker et al., 1994). *Ntl* in the tailbud helps

maintain axial progenitors by protecting them from premature differentiation induced by retinoic acid secreted by the anterior PSM and somites (Diez del Corral et al., 2003; Martin and Kimelman, 2010; Olivera-Martinez et al., 2012; Ribes et al., 2009).

Tailbud *Ntl* expression in *Greb1* morphants is indeed much lower than in wildtype or control embryos (M2: 20/34; MM: 0/11; Fig. 3Q',R,R'). Thus, *Greb1* is required for efficient *Ntl* expression, and reduced *Ntl* levels can explain the morphant embryos' truncated axis.

***Greb1* depletion affects somite polarity via the segmentation clock**

During axial segmentation in zebrafish embryos, a linear array of chevron-shaped somites is progressively generated from the PSM between 10-24 hpf (Fig. 3A,A'). As mentioned above, *Greb1* morphants lack morphologically discrete somites (Fig. 3A-C).

To assess if this morphological phenotype is accompanied by altered gene expression at somite boundaries, we examined *xirp2a/cb1045*, which is expressed in the myoseptum between myotomes (Deniziak et al., 2007; Schroter and Oates, 2010). Strong distinct posterior stripes of *Xirp2a* mRNA expression are frequently lost in *Greb1* morphant embryos (M1: 20/25; M2: 14/18; MM: 0/15; Fig. 3A-C), corresponding to the regions with abnormal somite appearance.

In wildtype embryos, boundaries arise between posterior and anterior compartments of adjacent somites, raising the possibility that *Greb1* is needed for somite compartmentalisation. To test this idea, we studied *myoD* transcripts, which are normally expressed in the posterior half of each somite (Weinberg et al., 1996). By contrast, expression of *myoD* extends into the anterior compartment in *Greb1* morphants (M1: 7/15; M2: 13/18; MM: 0/18; Fig. 3D-F), suggesting that anterior morphant cells have adopted a posterior character. M1

and M2 morphants show similar effects on axial morphology and *Xirp2a* and *myoD* expression, we only analysed M2 morphants in subsequent experiments.

Analysing *papC*, which is expressed in the anterior compartments of newly formed somites (Rhee et al., 2003) provides additional support for the idea that *Greb1* contributes to the establishment of anterior compartmentalisation. In morphant embryos, *papC* levels are reduced and lack clear borders (M2:14/22; MM:0/22 Fig. 3G,L).

Expression of *myoD* is normally suppressed in anterior somite compartments by *mespb* which together with *mespa*, is expressed there in newly-formed somites (Sawada et al., 2000). We examined expression of both *mesp* genes in the morphant embryos and found that, although *mespa* expression is not altered (M2: 0/24; MM:0/21 Fig. 3H,M), *mespb* expression is greatly lowered (M2: 6/10; MM: 0/21; Fig. 3 I,N). This reduction explains why *myoD* is derepressed in *Greb1* morphants, and reinforces our view that *Greb1* is needed for somite compartmentalisation.

What might cause mis-specification of somite compartments? During vertebrate axial extension, the regular production of equal-sized segments results from the action of a molecular oscillator ("segmentation clock"), which drives cyclic transcription of many PSM genes with a period corresponding to that of somite formation (Dequeant et al., 2006; Niwa et al., 2007; Palmeirim et al., 1997; Pourquie, 2011). Together, axial extension and cyclic gene expression establish reiterated expression of genes that define somite compartmentalisation and, hence, somite boundaries.

We examined two such cycling genes, *her1* and *her7*, which encode transcriptional repressors whose periodic expression in the zebrafish PSM form and pattern the somites (Oates and Ho, 2002; Pourquie, 2011; Takke and Campos-Ortega, 1999). In particular, *her7* is a regulator of *mespb* expression in

forming somites (Choorapoikayil et al., 2012; Oates and Ho, 2002). Expression of *her1* is normal in the PSMs of *Greb1* morphant embryos (M2 0/16; MM 0/19) Fig. 3 J,O), but that of *her7* is lost, in both the tailbud and PSM (M2 5/5; MM 0/5 Fig. 3 K,P). The latter's loss explains the reduced *mespb* expression and abnormal somite compartmentalisation in *Greb1* morphant embryos.

Together, our experiments support the following model for the *Greb1* morphant phenotypes (Fig. 3S). Axial extension is truncated due to reduced expression of *Ntl* and, thereby, loss of axial progenitors (Fig. 3Q,Q',R; Martin and Kimelman, 2010), and the segmentation phenotype is caused by loss of *her7*. This model is consistent with the misregulation of *mespb* and loss of more posterior somite boundaries in both *her7* mutants and *Greb1* morphants (Figs. 3A-F; A'-F'; Oates and Ho, 2002). Although we cannot completely exclude the possibility that the morphant morphological and molecular phenotypes are due to off-target knock-downs, this explanation seems unlikely. Each of the splice-blocking morpholinos was independently derived, and so they would not be expected affect similar sets of off-target transcripts. The combination of morphant phenotypes we observe has not previously been described, and we have also shown that they are not due to non-specific morphant toxicity. Future experiments using CRISPR/Cas9 gene-editing will clarify this point and allow further studies of *Greb1* action.

As *Greb1*, *Ntl* and *Her7* are all transcription factors, some of the effects on gene transcription that we observe may be direct. *Greb1* is required for clock output via *her7*, and may also act directly on *mespb*. However, the oscillator circuitry remains intact: morphants retain cyclic *her1* expression and low level, metameric *xirp2* expression (Fig. 3B,C,J,O). The latter idea would explain why *mespb* expression is abolished in the *Greb1* morphants (Fig 3I,N). Although further experiments will be required to distinguish between direct and indirect actions of *Greb1* and its potential targets, the evolutionarily conserved pattern and time-course of *Greb1* expression that we have shown in mouse, chick and zebrafish

(Fig. 2) suggest that *Greb1* is an important component in vertebrate axial patterning.

MATERIALS AND METHODS

Maintenance and collection of embryos

E10.5 mouse embryos were collected from *CD1* and *C57Bl/6J* pregnant females (Charles River Laboratories International, Inc. UK) in M2 media (Sigma Aldrich M7167). Fertilized chicken eggs from Henry Stewart & Co (Louth, UK) were incubated at 37°C, and embryos were staged according to Hamburger and Hamilton (Hamburger and Hamilton, 1992). Adult wild-type zebrafish were maintained at 27°C on a regular 14 h light/10 h dark cycle, and embryos were collected and staged as described by Kimmel et al. (Kimmel et al., 1995). *p53* heterozygous and homozygous mutant zebrafish embryos were obtained by crossing *p53* homozygous female to *p53* heterozygous males (Robu et al., 2007). Animals used in this study were handled by professionals meeting all the requirements of the Animals (Scientific Procedures) Act 1986.

Transcription profiling

Mouse CNH, PSM, and TBM explants per experiment were dissected as previously described (Fig. 1A; Cambray and Wilson, 2002). Approximately 50 pieces of each region were pooled, and total RNA extracted using the RNeasy Mini Kit (Qiagen Cat. No. 74104). Before processing the RNA samples for microarray analysis, their quality was tested using the Bioanalyser - RNA 6000 Pico kit (Agilent, Cat. No. 5067-1513). Samples with RNA integrity number (RIN) 8-10 were processed for transcriptional profiling at the Genome Centre (Barts and the London Medical School, Blizard Institute) using Illumina "Ref6v2" beads arrays. Two biological and one technical replicate were carried out for each region – CNH, TBM, and PSM.

Microarray data analysis

Analysis was performed using software packages developed for Bioconductor version 2.4.0 and R version 2.9.0. The Illumina dataset were processed using the probe intensity transformation (VST) and normalization (RSN) methods from the "lumi" package (Ihaka and Gentleman, 1996; Team, 2009).

Hierarchical clustering was used to assay the reproducibility of the biological replicates. Differential gene expression was assessed between tissue-type replicate groups using an empirical Bayes' t-test as implemented in the 'limma' package and taking account of replicate group and batch effects (K., 2005). Three comparisons were performed: CNH vs PSM, CNH vs TBM, CNH vs Combined PSM and TBM. The resulting p-values were adjusted to control the False Discovery Rate (FDR) using the Benjamini and Hochberg method. Two lists of differentially expressed genes were produced using different thresholds: 1) All genes that exhibited $FDR < 0.05$ in all three comparisons, or a fold change > 1.5 in the same direction in all three contrasts were classified as differentially expressed. 2) "Top50": Genes were selected on the basis of $FDR < 0.05$ and an absolute fold change ≥ 1.5 from the CNH vs PSM comparison, ordered by fold change, and the top 50 most-changed genes were selected and clustered using hierarchical clustering algorithm. Genes from the two lists were combined and used to perform a pathway enrichment and network analysis with MetaCore software from Clarivate Analytics.

In situ hybridisation

We visualised spatiotemporal transcript expression in mouse, chick and zebrafish embryos by in-situ hybridisation using digoxigenin-labelled antisense RNA probes (Hanisch et al., 2013; Rallis et al., 2010; Stauber et al., 2009). In general, templates for making antisense RNA probes for *in situ* detection of *Greb1* transcripts were generated by RT-PCR of embryonic mRNA, cloning into *PCR2.1-TOPO-TA* vector (Invitrogen; Table S5), linearisation using *Spe1* or *Not1*, and transcription by T3 or T7 RNA polymerase. cDNA templates for generating other antisense-RNA probes were obtained from the Julian Lewis lab. Expression patterns were replicated and scored independently by at least two people.

Morpholino injection

To knockdown zebrafish *Greb1* expression, we injected 2 nl of the following splicing-blocking morpholinos into 1-2 cell embryos at 2-8 ng/μl in 0.4 mM MgSO₄, 0.6 mM CaCl₂, 0.7 mM KCl, 58 mM NaCl, 5 mM HEPES pH 7.6; 0.05% phenol red: (M1) 5'-GGAAGACTGTAAAAGCTCACCCCTCA-3', (M2) 5'AATACTGAAATCACACCTCTCCTCC-3' (Fig. S1; Gene Tools, Philomath, Oregon, USA). Control injections used a mutated M2 oligo (MM) with 5 nucleotide mismatches: 5'-AATAGTCAAATCAGACCTGTGCTCC-3'. To test for non-specific toxicity, 4 ng/μl of blocking or control morpholino was co-injected with 6 ng/μl *p53* antisense morpholino (Robu et al., 2007). Efficacy and specificity were tested by sizing and sequencing RT-PCR products of total RNA from morpholino-injected embryos, SuperScript III One-Step RT-PCR mix (Invitrogen #12574035).

ACKNOWLEDGEMENTS

We thank the CR-UK Developmental Genetics Laboratory member, and Andrea Streit for comments on the paper. Val Wilson provided advice and training, generous help with CNH dissections, and key criticisms of a previous draft of the paper. The work was funded by Cancer Research UK and University College London.

DATA AND CODE AVAILABILITY

The non-normalised and normalized expression sequencing data and gene tables are available from the Gene Expression Omnibus (GEO) with accession number GSE141519.

AUTHOR CONTRIBUTIONS

R.S.P. and D.I.H. designed the project and wrote the paper. R.S.P performed most of the experiments. R.M. provided bioinformatics analysis; A.V. contributed to studying gene expression in chick and fish.

REFERENCES

- Brown, J. M. and Storey, K. G.** (2000). A region of the vertebrate neural plate in which neighbouring cells can adopt neural or epidermal fates. *Current biology : CB* **10**, 869-872.
- Cambray, N. and Wilson, V.** (2002). Axial progenitors with extensive potency are localised to the mouse chordoneural hinge. *Development* **129**, 4855-4866.
- (2007). Two distinct sources for a population of maturing axial progenitors. *Development* **134**, 2829-2840.
- Catala, M., Teillet, M. A., De Robertis, E. M. and Le Douarin, M. L.** (1996). A spinal cord fate map in the avian embryo: while regressing, Hensen's node lays down the notochord and floor plate thus joining the spinal cord lateral walls. *Development* **122**, 2599-2610.
- Choorapoikayil, S., Willems, B., Strohle, P. and Gajewski, M.** (2012). Analysis of her1 and her7 mutants reveals a spatio temporal separation of the somite clock module. *PLoS one* **7**, e39073.
- Deniziak, M., Thisse, C., Rederstorff, M., Hindelang, C., Thisse, B. and Lescure, A.** (2007). Loss of selenoprotein N function causes disruption of muscle architecture in the zebrafish embryo. *Exp Cell Res* **313**, 156-167.
- Dequeant, M. L., Glynn, E., Gaudenz, K., Wahl, M., Chen, J., Mushegian, A. and Pourquie, O.** (2006). A complex oscillating network of signaling genes underlies the mouse segmentation clock. *Science* **314**, 1595-1598.
- Diez del Corral, R., Olivera-Martinez, I., Goriely, A., Gale, E., Maden, M. and Storey, K.** (2003). Opposing FGF and retinoid pathways control ventral neural pattern, neuronal differentiation, and segmentation during body axis extension. *Neuron* **40**, 65-79.
- Du, P., Kibbe, W. A. and Lin, S. M.** (2008). lumi: a pipeline for processing Illumina microarray. *Bioinformatics* **24**, 1547-1548.
- Dunty, W. C., Jr., Kennedy, M. W., Chalamalasetty, R. B., Campbell, K. and Yamaguchi, T. P.** (2014). Transcriptional profiling of Wnt3a mutants identifies Sp transcription factors as essential effectors of the Wnt/beta-catenin pathway in neuromesodermal stem cells. *PLoS one* **9**, e87018.
- Finger, J. H., Smith, C. M., Hayamizu, T. F., McCright, I. J., Xu, J., Law, M., Shaw, D. R., Baldarelli, R. M., Beal, J. S., Blodgett, O., et al.** (2017). The mouse Gene Expression Database (GXD): 2017 update. *Nucleic acids research* **45**, D730-D736.
- Gouti, M., Delile, J., Stamataki, D., Wymeersch, F. J., Huang, Y., Kleinjung, J., Wilson, V. and Briscoe, J.** (2017). A Gene Regulatory Network Balances Neural and Mesoderm Specification during Vertebrate Trunk Development. *Developmental cell* **41**, 243-261 e247.

- Halpern, M. E., Ho, R. K., Walker, C. and Kimmel, C. B.** (1993). Induction of muscle pioneers and floor plate is distinguished by the zebrafish no tail mutation. *Cell* **75**, 99-111.
- Hamburger, V. and Hamilton, H. L.** (1992). A series of normal stages in the development of the chick embryo. 1951. *Developmental dynamics : an official publication of the American Association of Anatomists* **195**, 231-272.
- Hanisch, A., Holder, M. V., Choorapoikayil, S., Gajewski, M., Ozbudak, E. M. and Lewis, J.** (2013). The elongation rate of RNA polymerase II in zebrafish and its significance in the somite segmentation clock. *Development* **140**, 444-453.
- Ihaka, R. and Gentleman, R. R.** (1996). A Language for Data Analysis and Graphics. *Journal of Computational and Graphical Statistics*. **5**, 299–314.
- K., S. G. (2005).** “Limma: linear models for microarray data.” In Gentleman R, Carey V, Dudoit S, Irizarry R and Huber W (eds.), *Bioinformatics and Computational Biology Solutions Using R and Bioconductor*, pp. 397–420. Springer, New York .
- Kimmel, C. B., Ballard, W. W., Kimmel, S. R., Ullmann, B. and Schilling, T. F.** (1995). Stages of embryonic development of the zebrafish. *Developmental dynamics : an official publication of the American Association of Anatomists* **203**, 253-310.
- Lee, E., Wongvipat, J., Choi, D., Wang, P., Lee, Y. S., Zheng, D., Watson, P. A., Gopalan, A. and Sawyers, C. L.** (2019). GREB1 amplifies androgen receptor output in human prostate cancer and contributes to antiandrogen resistance. *Elife* **8**.
- Martin, B. L. and Kimelman, D.** (2010). Brachyury establishes the embryonic mesodermal progenitor niche. *Genes & development* **24**, 2778-2783.
- Maruoka, Y., Ohbayashi, N., Hoshikawa, M., Itoh, N., Hogan, B. L. and Furuta, Y.** (1998). Comparison of the expression of three highly related genes, Fgf8, Fgf17 and Fgf18, in the mouse embryo. *Mechanisms of development* **74**, 175-177.
- McGrew, M. J., Sherman, A., Lillico, S. G., Ellard, F. M., Radcliffe, P. A., Gilhooley, H. J., Mitrophanous, K. A., Cambray, N., Wilson, V. and Sang, H.** (2008). Localised axial progenitor cell populations in the avian tail bud are not committed to a posterior Hox identity. *Development* **135**, 2289-2299.
- Mohammed, H., D'Santos, C., Serandour, A. A., Ali, H. R., Brown, G. D., Atkins, A., Rueda, O. M., Holmes, K. A., Theodorou, V., Robinson, J. L., et al.** (2013). Endogenous purification reveals GREB1 as a key estrogen receptor regulatory factor. *Cell Rep* **3**, 342-349.
- Niwa, Y., Masamizu, Y., Liu, T., Nakayama, R., Deng, C. X. and Kageyama, R.** (2007). The initiation and propagation of Hes7 oscillation are

- cooperatively regulated by Fgf and notch signaling in the somite segmentation clock. *Developmental cell* **13**, 298-304.
- Oates, A. C. and Ho, R. K.** (2002). Hairy/E(spl)-related (Her) genes are central components of the segmentation oscillator and display redundancy with the Delta/Notch signaling pathway in the formation of anterior segmental boundaries in the zebrafish. *Development* **129**, 2929-2946.
- Olivera-Martinez, I., Harada, H., Halley, P. A. and Storey, K. G.** (2012). Loss of FGF-dependent mesoderm identity and rise of endogenous retinoid signalling determine cessation of body axis elongation. *PLoS Biol* **10**, e1001415.
- Olivera-Martinez, I., Schurch, N., Li, R. A., Song, J., Halley, P. A., Das, R. M., Burt, D. W., Barton, G. J. and Storey, K. G.** (2014). Major transcriptome re-organisation and abrupt changes in signalling, cell cycle and chromatin regulation at neural differentiation in vivo. *Development* **141**, 3266-3276.
- Palmeirim, I., Henrique, D., Ish-Horowicz, D. and Pourquie, O.** (1997). Avian hairy gene expression identifies a molecular clock linked to vertebrate segmentation and somitogenesis. *Cell* **91**, 639-648.
- Pourquie, O.** (2011). Vertebrate segmentation: from cyclic gene networks to scoliosis. *Cell* **145**, 650-663.
- Rallis, C., Pinchin, S. M. and Ish-Horowicz, D.** (2010). Cell-autonomous integrin control of Wnt and Notch signalling during somitogenesis. *Development* **137**, 3591-3601.
- Rhee, J., Takahashi, Y., Saga, Y., Wilson-Rawls, J. and Rawls, A.** (2003). The protocadherin papc is involved in the organization of the epithelium along the segmental border during mouse somitogenesis. *Developmental biology* **254**, 248-261.
- Ribes, V., Le Roux, I., Rhinn, M., Schuhbaur, B. and Dolle, P.** (2009). Early mouse caudal development relies on crosstalk between retinoic acid, Shh and Fgf signalling pathways. *Development* **136**, 665-676.
- Ritchie, M. E., Phipson, B., Wu, D., Hu, Y., Law, C. W., Shi, W. and Smyth, G. K.** (2015). limma powers differential expression analyses for RNA-sequencing and microarray studies. *Nucleic acids research* **43**, e47.
- Robu, M. E., Larson, J. D., Nasevicius, A., Beiraghi, S., Brenner, C., Farber, S. A. and Ekker, S. C.** (2007). p53 activation by knockdown technologies. *PLoS Genet* **3**, e78.
- Sawada, A., Fritz, A., Jiang, Y. J., Yamamoto, A., Yamasu, K., Kuroiwa, A., Saga, Y. and Takeda, H.** (2000). Zebrafish Mesp family genes, *mesp-a* and *mesp-b* are segmentally expressed in the presomitic mesoderm, and *Mesp-b* confers the anterior identity to the developing somites. *Development* **127**, 1691-1702.
- Schroter, C. and Oates, A. C.** (2010). Segment number and axial identity in a segmentation clock period mutant. *Current biology: CB* **20**, 1254-1258.

- Schulte-Merker, S., van Eeden, F. J., Halpern, M. E., Kimmel, C. B. and Nusslein-Volhard, C.** (1994). *no tail (ntl)* is the zebrafish homologue of the mouse *T (Brachyury)* gene. *Development* **120**, 1009-1015.
- Selleck, M. A. and Stern, C. D.** (1991). Fate mapping and cell lineage analysis of Hensen's node in the chick embryo. *Development* **112**, 615-626.
- Stauber, M., Sachidanandan, C., Morgenstern, C. and Ish-Horowicz, D.** (2009). Differential axial requirements for lunatic fringe and Hes7 transcription during mouse somitogenesis. *PloS one* **4**, e7996.
- Takada, S., Stark, K. L., Shea, M. J., Vassileva, G., McMahon, J. A. and McMahon, A. P.** (1994). Wnt-3a regulates somite and tailbud formation in the mouse embryo. *Genes & development* **8**, 174-189.
- Takke, C. and Campos-Ortega, J. A.** (1999). *her1*, a zebrafish pair-rule like gene, acts downstream of notch signalling to control somite development. *Development* **126**, 3005-3014.
- Tam, P. P. and Tan, S. S.** (1992). The somitogenetic potential of cells in the primitive streak and the tail bud of the organogenesis-stage mouse embryo. *Development* **115**, 703-715.
- Team, R. R. D. C.** (2009). R: A language and environment for statistical computing. R Foundation for Statistical Computing, Vienna, Austria. ISBN 3-900051-07-0, URL <http://www.R-project.org>.
- Tzouanacou, E., Wegener, A., Wymeersch, F. J., Wilson, V. and Nicolas, J. F.** (2009). Redefining the progression of lineage segregations during mammalian embryogenesis by clonal analysis. *Developmental cell* **17**, 365-376.
- Weinberg, E. S., Allende, M. L., Kelly, C. S., Abdelhamid, A., Murakami, T., Andermann, P., Doerre, O. G., Grunwald, D. J. and Riggelman, B.** (1996). Developmental regulation of zebrafish MyoD in wild-type, no tail and spadetail embryos. *Development* **122**, 271-280.
- Wilson, V. and Beddington, R. S.** (1996). Cell fate and morphogenetic movement in the late mouse primitive streak. *Mechanisms of development* **55**, 79-89.
- Wilson, V., Olivera-Martinez, I. and Storey, K. G.** (2009). Stem cells, signals and vertebrate body axis extension. *Development* **136**, 1591-1604.
- Wymeersch, F. J., Skylaki, S., Huang, Y., Watson, J. A., Economou, C., Marek-Johnston, C., Tomlinson, S. R. and Wilson, V.** (2019). Transcriptionally dynamic progenitor populations organised around a stable niche drive axial patterning. *Development* **146**. doi:10.1242/dev.168161
- Yamamoto, A., Amacher, S. L., Kim, S. H., Geissert, D., Kimmel, C. B. and De Robertis, E. M.** (1998). Zebrafish paraxial protocadherin is a downstream target of spadetail involved in morphogenesis of gastrula mesoderm. *Development* **125**, 3389-3397.

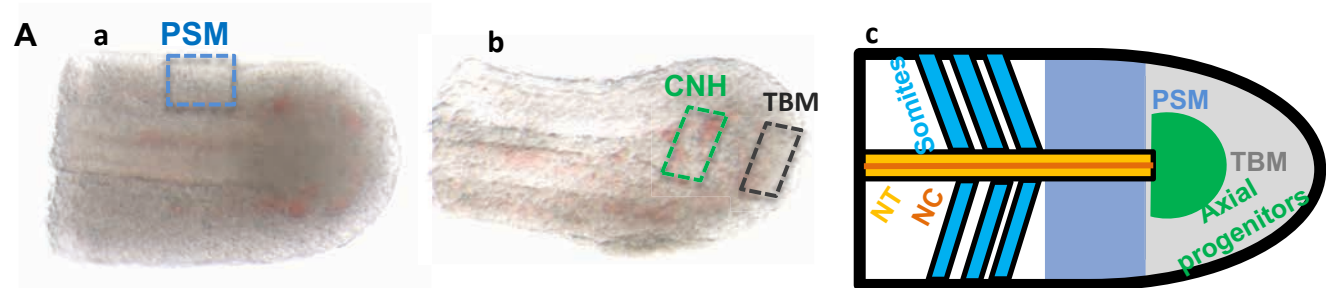
Zhang, J., Bai, S., Zhang, X., Nagase, H. and Sarras, M. P., Jr. (2003). The expression of gelatinase A (MMP-2) is required for normal development of zebrafish embryos. *Dev Genes Evol* **213**, 456-463

FIGURE LEGENDS

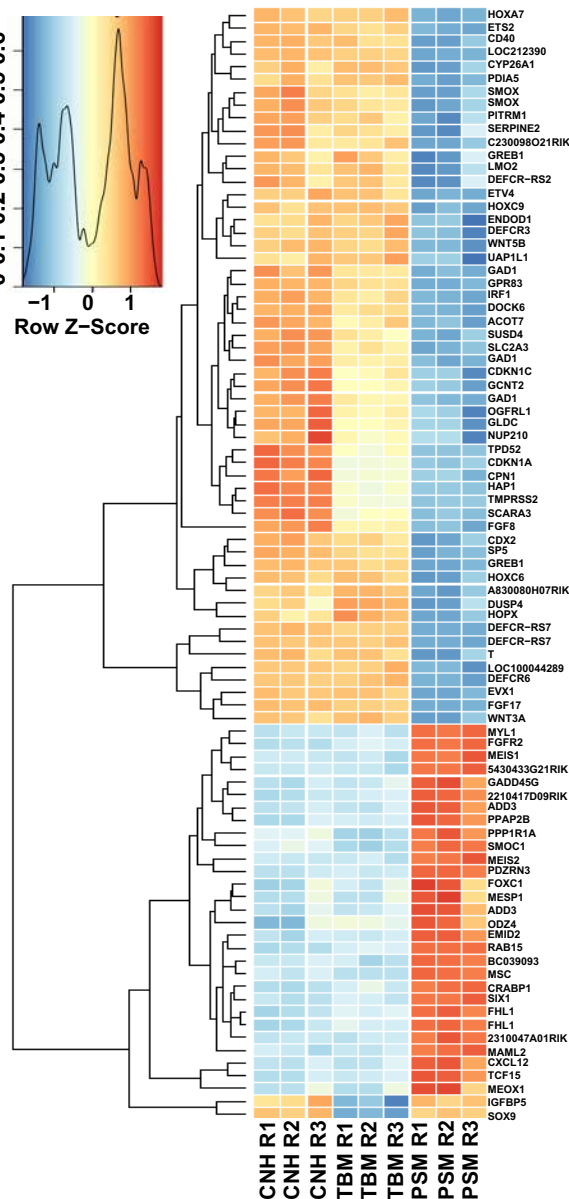
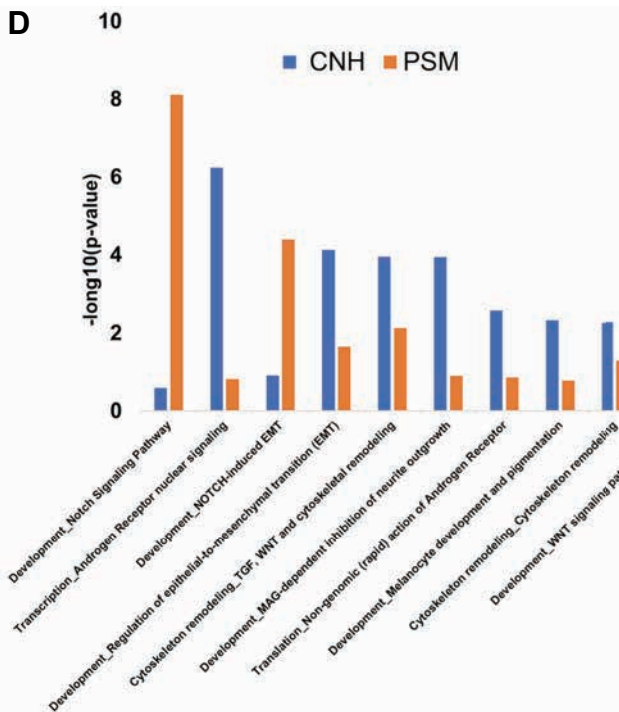
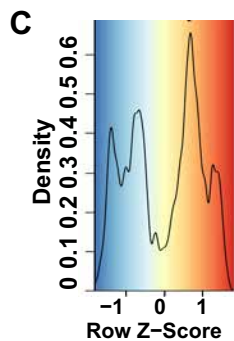
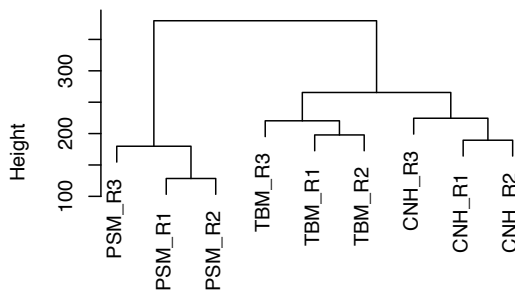
Fig. 1 CNH transcriptome is distinct from PSM. (A) Dissection of PSM, CNH, and TBM of mouse at E10.5; (a) dorsal view of E10.5 tail, black dotted rectangle represents dissected PSM and, (b) lateral view of (a) after removing PSM from last somite till end of tail; (c) schematic of tail regions with anterior to the left. Text colours correspond to those of different posterior axial regions colours (NT: neural tube; NC: notochord; PSM: presomitic mesoderm; TBM: tail bud mesoderm). Two biological and one technical replicates were performed for all three tissues (PSM, TBM and CNH). (B) A dendrogram illustrating the replicates' reproducibility, derived by hierarchical clustering of their transcriptomes (Supplementary Methods). (C) Heatmap showing differentially expressed genes (Fold change >2 and <-2, and p-value <0.05) in the CNH, TBM, and PSM. (D) Pathway enrichment analysis (see Supplementary Information). y-axis shows $-\log_{10}(\text{p-value})$ with enriched GO terms along the x-axis.

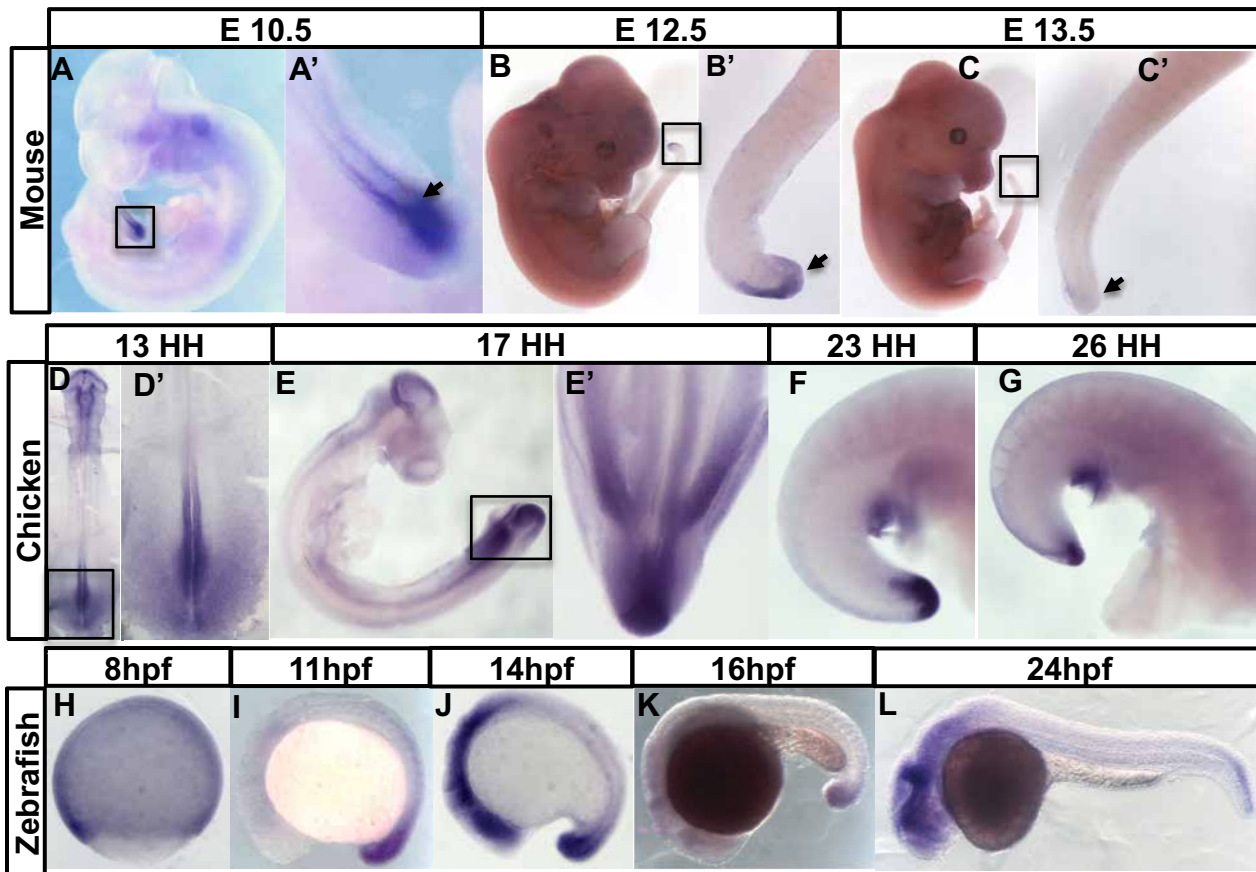
Fig. 2. The timing of axial *Greb1* expression is coincident with axial elongation in vertebrate embryos. (A–D) Mouse embryos and their tail regions at different embryonic stages. (A,A') Dorsal view of E8.5 embryo showing expression in the caudal lateral epiblast (CLE). PS: primitive streak. (B,B') Lateral view of E10.5 embryo, showing the *Greb1*-expressing tail region. (C) Lateral view of E12.5 tail region, showing reduced *Greb1* expression. (D) Lateral view of E13.5 tail region, showing that expression is lost. (E-F) *Greb1* expression in chick embryos at different stages: (E,E') dorsal views of HH13 embryo and its tail region; (F) is a lateral and (F') ventral view of a tail region at HH17; G is a lateral view of HH26 embryo, showing that *Greb1* expression in the tailbud is almost gone. H-L are lateral view of zebrafish embryos of the indicated ages (hpf=hours post-fertilisation). Each pattern was analysed in two independent experiments using, for each stage, at least 5 mouse, or 10-15 chicken or zebrafish embryos. Tailbud regions are arrowed. Boxes in lower magnification images show the tail regions with magnified views in the adjacent panel.

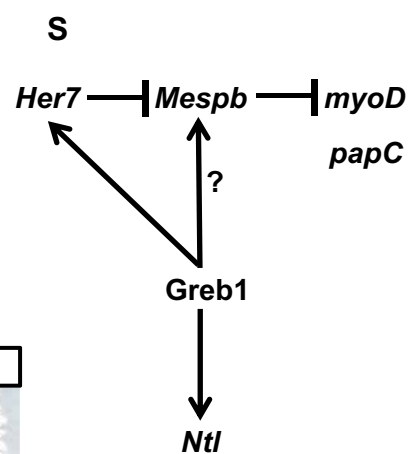
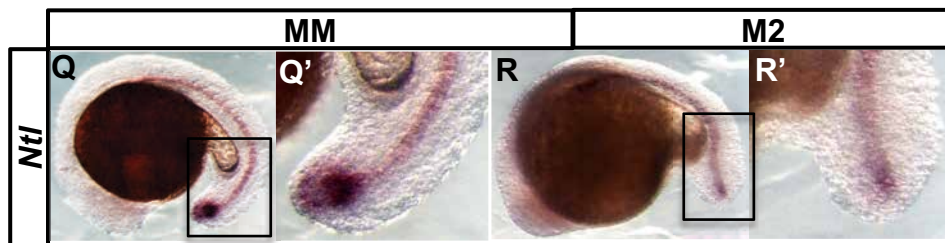
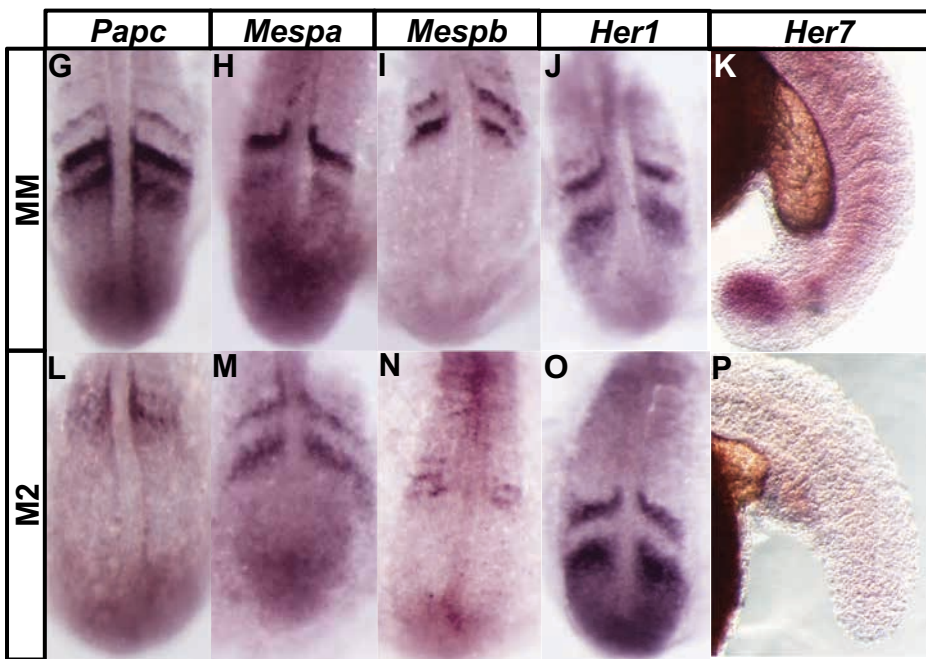
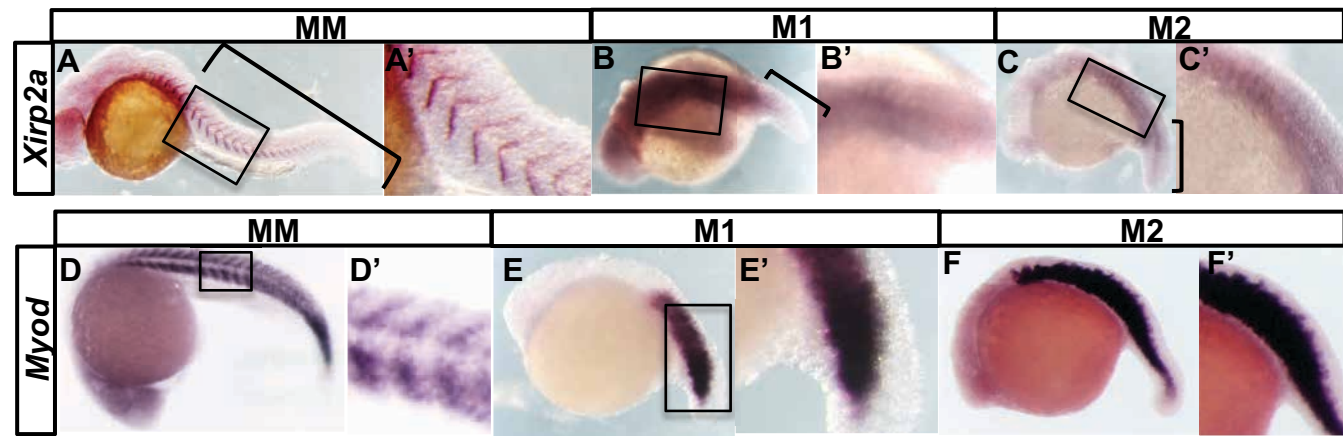
Fig. 3 *Greb1* is required for axial elongation. (A-C, A'-C'): lateral views of zebrafish embryos at 24 hpf, showing: (A) wildtype chevrons of *xirp2a* expression and the tail region (bracketed); (B, C) posterior loss in M1 and M2 morphants. The tail regions that are truncated and contain disrupted somites are bracketed. (D-F, D'-F'): expression of *myoD* in control (MM, M1 and M2 morphants). (G, L) *papc*; (H, M) *mespa*; (I, N) *mespb*; (J&O) *her1*; (K, P) *her7*; (Q, R) and (Q', R') *Ntl* expression in the tail region of 15 hpf control and morphant embryos. (S) shows a tentative model for gene interactions between *Greb1* and patterning genes. Anterior expression of *Her7* restricts *mespb* expression to the posterior somite compartment which, in turn, restricts *myoD* and *papC* expression to the anterior compartment. Continuous arrows indicate interactions shown by others as likely to be direct. Dashed arrows could be direct or indirect.



B Sample relations based on 45281 genes







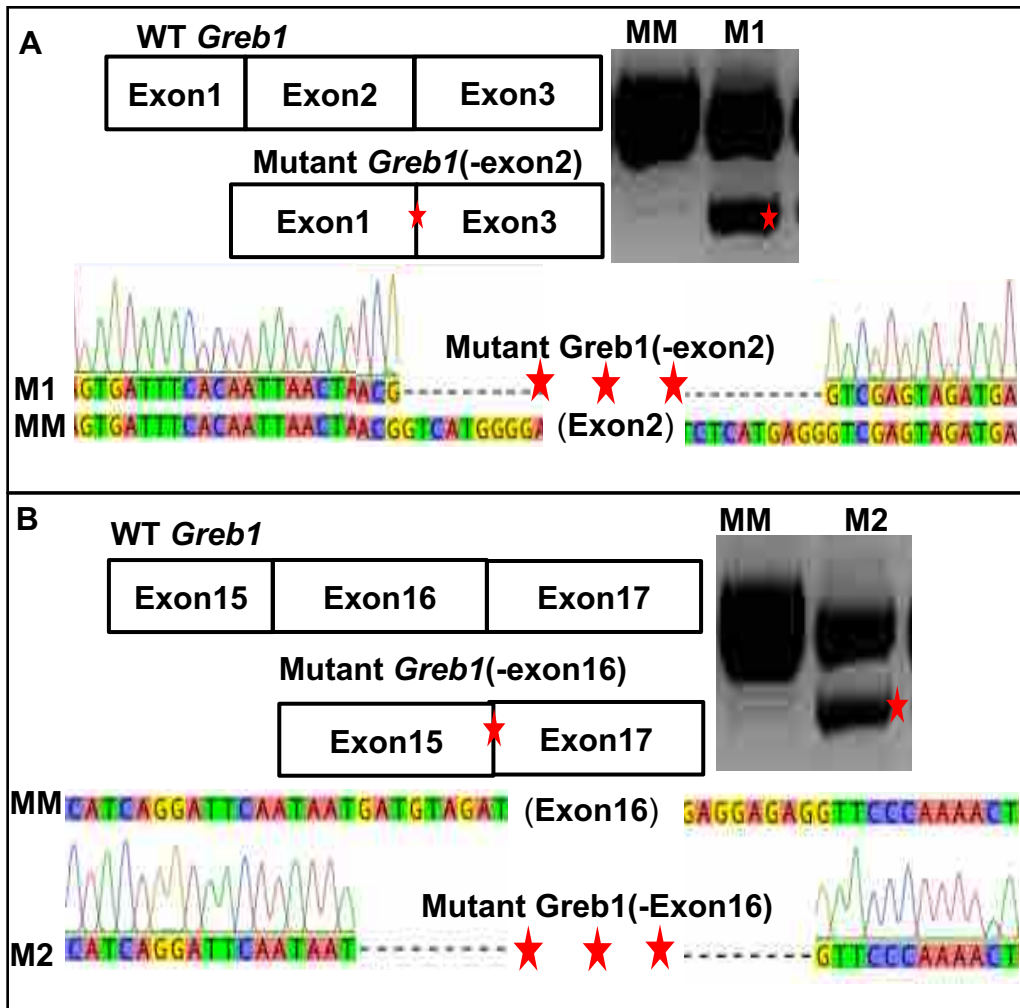


Figure S1

Table 1. List of differentially expressed genes in the CNH (FDR<0.01; Fold change >2 or <-2

ILMN_Gene	CNH vs PSM fold change	CNH vs PSM FDR	ILMN_Gene	CNH vs PSM fold change	CNH vs PSM FDR
DEFKR-RS7	11.9	1.96E-08	SCARA3	2.2	1.43E-06
T	10.2	6.68E-05	PDIA5	2.2	2.64E-05
FGF17	7.4	2.10E-09	ENDOD1	2.2	5.38E-04
LOC100044289	6.8	1.24E-05	NUP210	2.1	1.45E-03
WNT3A	6.0	1.62E-05	DEFKR3	2.1	1.23E-04
EVX1	6.0	6.83E-07	OGFRL1	2.1	3.55E-04
DEFKR6	5.1	1.09E-06	HOXC9	2.0	7.68E-06
FGF8	4.0	1.49E-06	HOXA11S	2.0	1.49E-06
GREB1	3.8	5.77E-07	CRIP2	2.0	9.04E-05
CDX2	3.8	3.03E-05	2610027C15RIK	2.0	4.67E-06
SP5	3.6	1.27E-06	Genes down regulated in the CNH		
HOXC6	3.6	4.54E-05	GPX2	-2.0	1.71E-05
A830080H07RIK	3.3	3.03E-05	EFNA5	-2.0	1.52E-06
ETS2	3.0	3.63E-07	SLC9A3R1	-2.0	1.42E-04
CPN1	2.9	3.52E-06	GADD45G	-2.0	1.05E-03
HOXA7	2.9	2.01E-06	2310047A01RIK	-2.1	1.52E-06
CDKN1A	2.7	3.63E-07	MESP1	-2.1	5.00E-03
DEFKR-RS2	2.7	5.49E-03	FHL1	-2.1	2.43E-06
TPD52	2.6	2.37E-06	CRABP1	-2.1	1.56E-06
CD40	2.6	2.91E-05	BC039093	-2.2	9.63E-06
LOC212390	2.6	7.02E-08	MSC	-2.2	1.03E-06
HOPX	2.5	1.07E-04	FOXC1	-2.2	5.53E-03
GAD1	2.5	3.25E-06	SIX1	-2.2	1.52E-06
GCNT2	2.5	1.71E-05	ADD3	-2.2	8.09E-04
C230098O21RIK	2.5	3.29E-04	SMOC1	-2.3	1.72E-06
GPR83	2.4	1.99E-07	EMID2	-2.5	1.90E-05
LMO2	2.4	8.26E-04	RAB15	-2.5	3.22E-08
DUSP4	2.4	2.03E-03	MAML2	-2.6	2.37E-06
ETV4	2.3	1.15E-05	PPP1R1A	-2.7	2.57E-05
DOCK6	2.3	1.12E-06	5430433G21RIK	-2.8	1.12E-06
TMPRSS2	2.3	1.21E-07	PPAP2B	-2.8	3.48E-05
IRF1	2.3	1.29E-06	MEIS1	-3.0	3.25E-06
SUSD4	2.3	1.98E-05	MYL1	-3.4	5.77E-07
SLC2A3	2.3	1.15E-06	2210417D09RIK	-3.4	3.25E-06
SMOX	2.3	6.56E-05	FGFR2	-3.7	5.07E-08
CDKN1C	2.3	1.03E-04	MEIS2	-4.0	3.25E-06
UAP1L1	2.3	1.67E-03	MEOX1	-4.7	5.31E-03
SERPINE2	2.3	4.93E-03	PDZRN3	-4.8	3.63E-07
CYP26A1	2.2	2.32E-04	CXCL12	-5.5	9.87E-05
GLDC	2.2	1.20E-04	TCF15	-5.8	2.09E-05
PITRM1	2.2	4.98E-04	ILMN_Gene CNH vs TBM.FC CNH vs TBM.FDR		
ACOT7	2.2	3.00E-05	IGFBP5	2.4	4.23E-03
HAP1	2.2	5.77E-07	SOX9	2.1	3.03E-05
WNT5B	2.2	1.01E-05			

Genes marked with * are differentially expressed in the CNH comparison to TBM and PSM (Fold change >1.5 or <=-1.5). Genes with FDR<0.01 and fold change >1.5 & <-1.5. The detailed data for all expression differences with FC >1.5 or <-1.5 are presented in the Table S1

Table 2. Annotated gene expression patterns (E7.5-13.5 mouse embryos) for genes that are differentially expressed in the CNH.

Gene	Anatomical regions
Gene up regulated in CNH > 2-fold change and FDR < -0.01	
Acot7	future spinal cord
Cdkn1a	neural tube, somite, dermomyotome, myotome, dermomyotome, somite, future spinal cord, somite
Cdkn1c	somite, dermomyotome, future spinal cord
Cdx2	tail bud, future spinal cord neural plate, neural tube, tail unsegmented mesenchyme, neural tube, tail mesenchyme
Cpn1	neural tube
Cyp26a1	future spinal cord neural plate, migrating neural crest, tail bud, tail mesenchyme, tail neural plate, tail neural tube, tail sclerotome
Dock6	future spinal cord, tail unsegmented mesenchyme
Dock7	somite
Dusp4	future spinal cord, tail unsegmented mesenchyme
Ets2	primitive streak, neural tube, somite, trunk somite, future spinal cord, tail unsegmented mesenchyme
Etv4	future spinal cord, primitive streak, future spinal cord neural plate, tail bud, dermomyotome, sclerotome, neural tube floor plate, future spinal cord
Evx1	primitive streak, primitive streak, primitive streak, primitive streak, tail bud, tail mesenchyme, future spinal cord, future spinal cord, neural tube, future spinal cord
Fgf8	future spinal cord, primitive streak, future spinal cord neural plate, somite, tail bud, trunk somite, tail mesenchyme, tail unsegmented mesenchyme, tail neural plate, trunk dermomyotome, myotome, tail somite, neural tube
fgf17	tail somite, somite, primitive streak, tail mesenchyme, tail unsegmented mesenchyme, neural tube
Gad1	neural tube, tail bud, tail mesenchyme, tail paraxial mesenchyme, tail future spinal cord, tail neural tube, future spinal cord
Gcnt2	future spinal cord
Gldc	neural lumen
Greb1	future spinal cord
Hopx	tail unsegmented mesenchyme and neural tube basal columns
Hoxa7	neural tube ventricular layer, trunk somite, somite, neural tube, tail paraxial mesenchyme
Hoxc6	neural tube, somite, primitive streak, trunk somite
Hoxc9	tail paraxial mesenchyme, neural tube, trunk somite, tail somite
Lmo2	Neural tube and Head somites
Pitrm1	somite and neural tube
Serpine2	trunk dermomyotome and neural tube
Slc2a3	neural tube
Sp5	future spinal cord, somite, primitive streak, head somite, trunk somite, future spinal cord neural plate, neural tube, tail unsegmented mesenchyme, dermomyotome, tail somite, neural tube lateral wall, tail mesenchyme
T	dermomyotome, primitive streak, node, future spinal cord neural plate, tail neural tube, tail bud, tail mesenchyme, tail unsegmented mesenchyme, tail neural plate, caudal neuropore, neural tube
Wnt3a	tail bud, primitive streak, future spinal cord, tail mesenchyme, tail unsegmented mesenchyme, neural tube, neural tube roof plate, neural tube lateral wall, sclerotome, neural tube floor plate
Wnt5b	neural tube floor plate, futrue spinal cord, neural tube

Genes down regulated in CNH < -2-fold change FDR < -0.01

Add3	tail unsegmented mesenchyme
Cfh	future spinal cord
Crabp1	neural crest, neural tube, head somite, trunk somite, migrating neural crest, trunk sclerotome, neural tube lateral wall, future spinal cord, primitive streak, trunk unsegmented mesenchyme, anterior pro-rhombomere neural crest, future hindbrain posterior to rhombomere 5 neural crest, posterior pro-rhombomere neural crest, rhombomere 1 neural crest, rhombomere 2 neural crest, rhombomere 5 neural crest, future spinal cord neural fold, neural tube floor plate, future midbrain neural crest, future diencephalon neural crest, prosencephalon neural crest, tail bud, trunk dermomyotome, somite, neural tube roof plate
Cxcl12	future spinal cord
Fgfr2	primitive streak, head somite, trunk somite, neural tube, neural tube lateral wall, myotome, sclerotome
Foxc1	primitive streak, node, future spinal cord, trunk paraxial mesenchyme, head somite, trunk somite, trunk unsegmented mesenchyme, neural tube, somite, tail unsegmented mesenchyme, trunk dermomyotome, trunk sclerotome, tail sclerotome
Gadd45g	trunk unsegmented mesenchyme, neural fold, trunk unsegmented mesenchyme, future spinal cord neural fold, tail unsegmented mesenchyme, neural tube, tail unsegmented mesenchyme, myotome, neural tube
Ism1	somite, trunk unsegmented mesenchyme, somite, somite, tail unsegmented mesenchyme, neural tube, dermomyotome
Maml2	neural tube
Meis1	trunk somite, future spinal cord, trunk paraxial mesenchyme, somite, neural plate, neural fold, neural groove, trunk unsegmented mesenchyme, neural tube, trunk myotome, trunk sclerotome, myotome, sclerotome, neural tube floor plate, neural tube mantle layer
Meis2	neural plate, neural fold, neural groove, trunk unsegmented mesenchyme, neural tube, somite, future spinal cord, trunk somite, trunk myotome, trunk sclerotome, myotome, sclerotome, neural tube floor plate, neural tube mantle layer
Meox1	primitive streak, trunk paraxial mesenchyme, head somite, trunk somite, trunk unsegmented mesenchyme, somite, dermomyotome, sclerotome, trunk dermomyotome, trunk sclerotome, trunk myotome, neural tube, tail somite, tail unsegmented mesenchyme, unsegmented mesenchyme
Mesp1	primitive streak, trunk unsegmented mesenchyme, tail unsegmented mesenchyme, trunk somite
Msc	trunk and tail dermomyotome
Myl1	somite, myotome, trunk somite, tail paraxial mesenchyme
Pdzn3	tail somite, tail unsegmented mesenchyme
Plpp3	neural tube ventricular layer, Somite, myotome
Ppp1r1a	neural tube, , node, somite
Rab15	neural tube
Six1	trunk somite, trunk unsegmented mesenchyme, tail unsegmented mesenchyme, somite
Smoc1	node, somite, primitive streak
Tcf15	primitive streak, head somite, trunk paraxial mesenchyme, trunk unsegmented mesenchyme, trunk somite, somite, tail paraxial mesenchyme, tail unsegmented mesenchyme, dermatome, myotome, sclerotome, tail sclerotome, trunk dermomyotome, dermomyotome, trunk sclerotome
Tenm4	future brain neural fold, future spinal cord neural plate, future spinal cord neural fold, trunk somite, somite, tail somite

Expression patterns were extracted from the Mouse Genome Informatics (MGI) database. Details of the data, including references, are reported in Table S2

ILMN_Gene	CNH_Vs_PSM .FDR	CNH_Vs_PSM.FC	CNH_Vs_TBM.FC	CNH_Vs_TBM. FDR	Probe_Id
DEFKR-RS7	1.96E-08	11.9	1.2	0.093	ILMN_2524945
T	6.68E-05	10.2	1.1	0.905	ILMN_1244340
FGF17	2.10E-09	7.4	1.2	0.025	ILMN_2812286
LOC10004428	1.24E-05	6.8	-1.0	0.990	ILMN_1231270
WNT3A	1.62E-05	6.0	-1.1	0.770	ILMN_1220516
EVX1	6.83E-07	6.0	1.0	0.894	ILMN_2731113
DEFKR6	1.09E-06	5.1	-1.1	0.800	ILMN_1254739
FGF8	1.49E-06	4.0	1.7	0.004	ILMN_2721370
GREB1	5.77E-07	3.8	1.1	0.294	ILMN_2433318
CDX2	3.03E-05	3.8	1.3	0.353	ILMN_2725853
SP5	1.27E-06	3.6	1.3	0.085	ILMN_2641201
HOXC6	4.54E-05	3.6	1.0	0.987	ILMN_1217328
A830080H07R	3.03E-05	3.3	-1.2	0.480	ILMN_2457437
ETS2	3.63E-07	3.0	1.2	0.084	ILMN_2594714
CPN1	3.52E-06	2.9	1.9	0.002	ILMN_1253362
HOXA7	2.01E-06	2.9	1.0	0.870	ILMN_2621038
CDKN1A	3.63E-07	2.7	1.9	0.000	ILMN_2634083
DEFKR-RS2	5.49E-03	2.7	1.1	0.932	ILMN_1231872
TPD52	2.37E-06	2.6	1.7	0.002	ILMN_3091288
CD40	2.91E-05	2.6	1.1	0.534	ILMN_3115796
LOC212390	7.02E-08	2.6	1.1	0.140	ILMN_1240069
HOPX	1.07E-04	2.5	-1.3	0.160	ILMN_2548010
GAD1	3.25E-06	2.5	1.3	0.041	ILMN_1234988
GCNT2	1.71E-05	2.5	1.5	0.015	ILMN_1227951
C230098O21R	3.29E-04	2.5	1.1	0.650	ILMN_2420353
GPR83	1.99E-07	2.4	1.2	0.020	ILMN_2707941
LMO2	8.26E-04	2.4	1.0	0.997	ILMN_2767605
DUSP4	2.03E-03	2.4	-1.4	0.368	ILMN_2450767
ETV4	1.15E-05	2.3	1.0	0.802	ILMN_2778111
DOCK6	1.12E-06	2.3	1.2	0.044	ILMN_2760963
TMPRSS2	1.21E-07	2.3	1.7	0.000	ILMN_1223880
IRF1	1.29E-06	2.3	1.2	0.034	ILMN_2834777
SUSD4	1.98E-05	2.3	1.3	0.041	ILMN_2677824
SLC2A3	1.15E-06	2.3	1.3	0.008	ILMN_2616565
SMOX	6.56E-05	2.3	1.2	0.317	ILMN_1247267
CDKN1C	1.03E-04	2.3	1.4	0.070	ILMN_2708203
UAP1L1	1.67E-03	2.3	-1.1	0.767	ILMN_2467800
SERPINE2	4.93E-03	2.3	1.2	0.742	ILMN_1246808
CYP26A1	2.32E-04	2.2	-1.1	0.805	ILMN_2957054
GLDC	1.20E-04	2.2	1.4	0.054	ILMN_2873750
PITRM1	4.98E-04	2.2	1.2	0.585	ILMN_2780167
ACOT7	3.00E-05	2.2	1.2	0.123	ILMN_2632264
SCARA3	1.43E-06	2.2	1.5	0.001	ILMN_2706268
HAP1	5.77E-07	2.2	1.6	0.000	ILMN_1244829
WNT5B	1.01E-05	2.2	1.0	0.758	ILMN_1224193
PDIA5	2.64E-05	2.2	-1.1	0.794	ILMN_1255177
ENDOD1	5.38E-04	2.2	-1.1	0.905	ILMN_2733356
NUP210	1.45E-03	2.1	1.4	0.191	ILMN_1257579
DEFKR3	1.23E-04	2.1	-1.0	0.886	ILMN_2524832

OGFRL1	3.55E-04	2.1	1.3	0.161	ILMN_1236107
HOXC9	7.68E-06	2.0	-1.0	0.780	ILMN_2772764
HOXA11S	1.49E-06	2.0	-1.1	0.370	ILMN_2619975
CRIP2	9.04E-05	2.0	1.2	0.170	ILMN_2710449
2610027C15R	4.67E-06	2.0	-1.1	0.651	ILMN_2890357
RAB8B	1.72E-03	1.9	-1.2	0.501	ILMN_1223029
SLIT2	2.01E-06	1.9	1.1	0.543	ILMN_1253797
3000003G13R	3.38E-05	1.9	1.4	0.022	ILMN_2551723
HOXB7	2.09E-05	1.9	1.2	0.183	ILMN_2946183
MGST1	4.81E-03	1.9	-1.1	0.871	ILMN_2940195
HBB-B1	2.67E-02	1.9	1.0	0.964	ILMN_1255462
LOC10004586	2.91E-05	1.9	1.1	0.294	ILMN_2535306
SALL3	1.31E-04	1.9	1.2	0.237	ILMN_1252794
AY761185	3.26E-03	1.9	-1.0	0.995	ILMN_2903718
RSPO3	3.40E-04	1.9	-1.2	0.422	ILMN_3162785
SNX11	1.96E-05	1.8	1.0	0.736	ILMN_2674752
FURIN	1.03E-06	1.8	1.1	0.077	ILMN_3148489
RNF208	2.62E-05	1.8	1.3	0.030	ILMN_2636349
CCND1	3.85E-05	1.8	1.1	0.711	ILMN_2601471
TCEA3	3.25E-06	1.8	1.4	0.002	ILMN_2776283
HOXC10	1.05E-02	1.8	-1.1	0.823	ILMN_2836888
ENO3	5.03E-06	1.8	1.2	0.044	ILMN_2757569
PRNP	1.41E-03	1.8	1.1	0.838	ILMN_2619316
PGM2	3.58E-05	1.8	1.0	0.771	ILMN_1230977
PRR18	1.49E-06	1.8	1.0	0.585	ILMN_2728682
DEFCR26	6.98E-04	1.8	-1.0	0.981	ILMN_2938932
2310007H09R	4.59E-03	1.8	1.2	0.641	ILMN_2600720
WFDC2	9.95E-05	1.8	1.3	0.030	ILMN_1236758
1200009O22R	2.43E-06	1.8	1.1	0.217	ILMN_2615431
NGFR	1.42E-04	1.8	-1.3	0.050	ILMN_2851288
FNBP1	9.54E-04	1.7	-1.1	0.567	ILMN_1255974
SBK	1.13E-06	1.7	1.3	0.002	ILMN_2724545
HOXD10	5.26E-05	1.7	1.1	0.550	ILMN_2702687
SLC1A4	8.90E-06	1.7	-1.0	0.876	ILMN_2888552
ZCCHC18	4.96E-04	1.7	1.4	0.053	ILMN_2649172
LOC10004417	2.27E-05	1.7	1.0	0.942	ILMN_1232495
SGK1	2.41E-03	1.7	-1.1	0.848	ILMN_1213954
OAT	1.89E-02	1.7	1.1	0.749	ILMN_2933112
1110007M04F	1.47E-03	1.7	1.2	0.356	ILMN_2734060
ADAMTSL2	1.72E-04	1.7	-1.1	0.737	ILMN_2650115
FZD10	1.11E-04	1.7	1.1	0.372	ILMN_2976821
GRINA	6.44E-05	1.7	1.4	0.012	ILMN_2588411
TRIM2	2.46E-04	1.7	1.1	0.650	ILMN_2511355
NOTUM	4.28E-03	1.7	1.2	0.344	ILMN_2932164
CD83	5.06E-05	1.7	1.1	0.332	ILMN_2865016
CD63	5.83E-04	1.7	-1.2	0.187	ILMN_2653617
D17WSU92E	1.52E-03	1.7	-1.2	0.267	ILMN_1257938
APCDD1	9.43E-03	1.7	1.0	0.948	ILMN_2965660
ADRB2	1.01E-03	1.7	1.3	0.125	ILMN_1241610
GABARAPL1	2.24E-05	1.7	1.1	0.149	ILMN_1236958
ANXA3	4.98E-04	1.7	1.1	0.747	ILMN_3135781
ZYX	1.84E-05	1.7	1.0	0.802	ILMN_2514292

SCARA5	4.28E-03	1.6	1.0	0.896	ILMN_3008068
D630014A15R	1.71E-04	1.6	1.1	0.664	ILMN_1242794
OLFML3	2.73E-06	1.6	1.1	0.069	ILMN_1233455
CIB1	3.04E-04	1.6	-1.0	0.991	ILMN_2621847
IL17RD	3.02E-05	1.6	1.0	0.742	ILMN_1248657
RAMP2	5.22E-04	1.6	1.3	0.044	ILMN_2661422
NOTCH4	2.93E-04	1.6	-1.0	0.978	ILMN_1220697
SLC1A3	2.47E-03	1.6	-1.1	0.810	ILMN_2634317
LYPD6B	1.00E-04	1.6	1.2	0.164	ILMN_2596998
SAMD9L	2.73E-02	1.6	1.3	0.516	ILMN_1224855
PGK1	9.39E-04	1.6	-1.0	0.861	ILMN_2651886
TPM1	1.20E-02	1.6	-1.1	0.741	ILMN_3007072
LOC10004677	2.22E-04	1.6	-1.0	0.986	ILMN_1225654
ELF3	4.56E-03	1.6	1.1	0.824	ILMN_2850233
CENTD3	3.50E-03	1.6	1.1	0.725	ILMN_1243107
ACOT1	1.77E-04	1.6	1.4	0.019	ILMN_3139875
CHST7	1.31E-04	1.6	-1.4	0.013	ILMN_1216374
LIX1	5.03E-06	1.6	1.1	0.044	ILMN_2686594
C230082I21RI	1.82E-05	1.6	-1.1	0.192	ILMN_1248824
BEX4	2.89E-03	1.6	1.3	0.153	ILMN_3043587
BIK	1.01E-03	1.6	1.2	0.187	ILMN_2717011
CRELD1	1.90E-05	1.6	1.2	0.031	ILMN_1232170
A630082K20R	1.55E-04	1.6	1.2	0.128	ILMN_2595814
HBA-X	2.27E-03	1.6	1.1	0.477	ILMN_1240267
DEFKR-RS10	1.04E-03	1.6	1.0	0.948	ILMN_2746576
LY6A	2.08E-03	1.6	1.2	0.416	ILMN_1255416
THSD2	3.21E-03	1.6	-1.1	0.649	ILMN_2736451
SCT	9.98E-04	1.6	-1.8	0.003	ILMN_2592834
MMP2	8.69E-05	1.6	1.1	0.654	ILMN_2678218
DUSP6	1.54E-02	1.6	1.1	0.885	ILMN_2925711
RPS6KA1	1.24E-05	1.6	1.1	0.416	ILMN_2975718
FOXA3	2.79E-02	1.6	1.4	0.317	ILMN_1228748
B930075F07	4.31E-04	1.6	1.0	0.945	ILMN_1247127
DDAH1	9.94E-05	1.5	1.2	0.058	ILMN_1256676
GJA1	5.79E-03	1.5	-1.1	0.750	ILMN_1244291
KLHL6	6.56E-05	1.5	1.2	0.036	ILMN_2619528
ETSRP71	1.36E-04	1.5	1.1	0.315	ILMN_2678641
LIMCH1	1.01E-05	1.5	-1.0	0.936	ILMN_2628603
5830411I20	1.01E-03	1.5	1.0	0.925	ILMN_2474052
SHC1	8.26E-05	1.5	1.0	0.839	ILMN_2957070
MYLC2B	1.14E-03	1.5	1.2	0.304	ILMN_2953531
RASGRP4	1.74E-04	1.5	1.0	0.847	ILMN_1228808
HOXD12	4.16E-04	1.5	-1.1	0.398	ILMN_2951852
CAR14	1.08E-02	1.5	-1.1	0.682	ILMN_2973824
ANGPT2	1.23E-04	1.5	1.0	0.941	ILMN_1234487
RELL1	3.91E-05	1.5	-1.1	0.300	ILMN_2656645
IAP	3.65E-04	1.5	1.0	0.815	ILMN_1225712
SHH	2.92E-03	1.5	1.4	0.041	ILMN_2610013
LOC10004541	9.61E-03	1.5	1.0	0.907	ILMN_1245007
LAMA1	3.60E-05	-1.5	-1.3	0.011	ILMN_2973288
FZD7	8.09E-04	-1.5	-1.2	0.284	ILMN_2907560
CRHBP	9.04E-06	-1.5	1.0	0.995	ILMN_1231710

TMSB10	2.20E-03	-1.5	-1.0	0.934	ILMN_3067068
LRN1	2.44E-05	-1.5	-1.0	0.901	ILMN_2759736
RASGRP1	2.37E-06	-1.5	-1.0	0.917	ILMN_1246609
SULF1	3.71E-05	-1.5	-1.0	0.620	ILMN_2501191
PHF17	3.59E-04	-1.5	1.1	0.592	ILMN_2707137
IRF6	4.71E-06	-1.5	-1.0	0.473	ILMN_1216279
PPIB	1.07E-04	-1.5	-1.0	0.918	ILMN_1245092
RBM35A	4.63E-03	-1.5	1.0	0.913	ILMN_2947559
UCK2	3.65E-04	-1.5	-1.0	0.889	ILMN_2880536
MYOCD	5.55E-03	-1.5	-1.0	0.945	ILMN_2435360
PEG3	6.51E-03	-1.5	1.0	0.977	ILMN_1245246
DDIT4L	6.61E-05	-1.6	1.2	0.101	ILMN_2695819
LOC671878	4.69E-04	-1.6	-1.1	0.379	ILMN_1217489
MLLT4	2.50E-03	-1.6	-1.0	0.991	ILMN_2593230
ODZ4	1.72E-02	-1.6	-1.2	0.526	ILMN_1230926
METR1	1.25E-05	-1.6	-1.1	0.281	ILMN_2739843
CLIC4	8.77E-04	-1.6	-1.3	0.072	ILMN_1230546
1600021P15R	1.15E-05	-1.6	-1.1	0.248	ILMN_2453954
CAMK2N1	2.73E-06	-1.6	1.0	0.534	ILMN_2810963
NKD2	1.52E-03	-1.6	-1.3	0.143	ILMN_1228631
SYNM	8.90E-04	-1.6	1.0	0.922	ILMN_1214880
ZNF512B	3.42E-05	-1.6	1.1	0.462	ILMN_1219778
IFITM1	2.05E-06	-1.6	-1.1	0.102	ILMN_1214071
FRMD6	1.45E-05	-1.6	-1.2	0.048	ILMN_2828916
TUBB2B	2.81E-05	-1.6	1.2	0.052	ILMN_1377919
COL5A1	9.87E-05	-1.6	-1.0	0.879	ILMN_2748402
SAP30	5.08E-04	-1.6	1.0	0.895	ILMN_2694917
NME7	4.51E-06	-1.6	-1.3	0.002	ILMN_1259075
PCDH19	5.09E-03	-1.6	1.0	0.998	ILMN_2696829
PGM5	5.96E-04	-1.6	1.0	0.979	ILMN_3129198
FGF18	3.95E-03	-1.6	-1.0	0.987	ILMN_2764004
LRIG1	1.95E-04	-1.6	1.0	0.927	ILMN_2640862
NRARP	3.04E-04	-1.6	-1.0	0.972	ILMN_2596979
4732462B05R	7.79E-05	-1.6	1.2	0.101	ILMN_1213708
IFITM3	3.55E-04	-1.7	-1.1	0.596	ILMN_2658501
DAB2IP	1.67E-04	-1.7	-1.1	0.579	ILMN_2615557
GMDS	1.04E-06	-1.7	-1.0	0.586	ILMN_2766596
TCF3	1.52E-02	-1.7	-1.1	0.926	ILMN_3109289
F830002E14RI	5.00E-03	-1.7	-1.5	0.086	ILMN_1215076
LOC10004548	1.15E-06	-1.7	-1.1	0.104	ILMN_1213311
4631426J05RI	5.74E-05	-1.7	1.0	0.803	ILMN_1239627
SPSB4	2.29E-05	-1.7	1.0	0.876	ILMN_1243507
LRIG3	1.95E-05	-1.7	-1.1	0.279	ILMN_1213273
PDLIM1	2.87E-06	-1.7	-1.1	0.443	ILMN_1234072
RBP1	2.43E-06	-1.7	-1.0	0.519	ILMN_1238433
LOC10004696	5.38E-04	-1.7	-1.0	0.968	ILMN_1220560
NOTCH1	2.07E-05	-1.7	1.0	0.738	ILMN_1241915
1110014O20R	1.07E-04	-1.7	1.1	0.391	ILMN_1233987
IGSF4A	1.93E-04	-1.8	-1.1	0.759	ILMN_2505841
LHFPL2	1.47E-05	-1.8	1.0	0.977	ILMN_2721357
ZFP238	2.01E-06	-1.8	-1.1	0.167	ILMN_3124947
TRP63	2.01E-06	-1.8	-1.1	0.336	ILMN_1216742

PTN	1.62E-05	-1.8	1.2	0.042	ILMN_2638114
VSTM2B	1.31E-05	-1.8	-1.0	0.877	ILMN_1251276
EPB4.1L3	3.81E-04	-1.8	-1.1	0.754	ILMN_1244272
COL18A1	4.59E-04	-1.8	1.2	0.250	ILMN_2735184
PHXR4	3.59E-04	-1.8	-1.0	0.876	ILMN_2751603
CER1	4.85E-03	-1.8	-1.0	0.953	ILMN_2775793
HS3ST3A1	2.01E-06	-1.8	-1.0	0.543	ILMN_2627193
LMO4	1.20E-04	-1.9	-1.3	0.072	ILMN_2642403
RIPPLY2	1.90E-02	-1.9	1.0	0.991	ILMN_1250174
KRT14	5.77E-07	-1.9	-1.0	0.673	ILMN_2722616
CITED2	3.43E-04	-1.9	-1.0	0.872	ILMN_2477221
LOC10004623	2.23E-05	-1.9	-1.0	0.792	ILMN_2595732
FOXC2	2.27E-07	-1.9	-1.0	0.726	ILMN_2703433
RELN	7.65E-06	-1.9	-1.0	0.922	ILMN_2704257
GPX2	1.71E-05	-2.0	-1.0	0.971	ILMN_2674483
EFNA5	1.52E-06	-2.0	1.0	0.926	ILMN_2757641
SLC9A3R1	1.42E-04	-2.0	1.0	0.881	ILMN_1240256
GADD45G	1.05E-03	-2.0	-1.0	0.926	ILMN_2744890
2310047A01R	1.52E-06	-2.1	-1.0	0.987	ILMN_2675922
MESP1	5.00E-03	-2.1	-1.0	0.986	ILMN_2687727
FHL1	2.43E-06	-2.1	-1.1	0.153	ILMN_2713285
CRABP1	1.56E-06	-2.1	-1.1	0.160	ILMN_1227671
BC039093	9.63E-06	-2.2	1.1	0.617	ILMN_2738156
MSC	1.03E-06	-2.2	1.1	0.324	ILMN_2769777
FOXC1	5.53E-03	-2.2	-1.1	0.920	ILMN_2886260
SIX1	1.52E-06	-2.2	-1.1	0.453	ILMN_2904117
ADD3	8.09E-04	-2.2	-1.0	0.932	ILMN_2901283
SMOC1	1.72E-06	-2.3	1.3	0.021	ILMN_1225376
EMID2	1.90E-05	-2.5	-1.1	0.774	ILMN_1247358
RAB15	3.22E-08	-2.5	-1.2	0.008	ILMN_1217009
MAML2	2.37E-06	-2.6	-1.0	0.887	ILMN_2457571
PPP1R1A	2.57E-05	-2.7	1.4	0.060	ILMN_2616584
5430433G21R	1.12E-06	-2.8	1.0	0.714	ILMN_2728134
PPAP2B	3.48E-05	-2.8	-1.1	0.709	ILMN_2630993
MEIS1	3.25E-06	-3.0	1.1	0.688	ILMN_1218266
MYL1	5.77E-07	-3.4	-1.0	0.885	ILMN_2878542
2210417D09R	3.25E-06	-3.4	-1.1	0.480	ILMN_2594066
FGFR2	5.07E-08	-3.7	-1.2	0.023	ILMN_1225071
MEIS2	3.25E-06	-4.0	1.0	0.877	ILMN_2850391
MEOX1	5.31E-03	-4.7	1.0	0.978	ILMN_1213886
PDZRN3	3.63E-07	-4.8	-1.1	0.560	ILMN_3156010
CXCL12	9.87E-05	-5.5	-1.0	0.975	ILMN_2658908
TCF15	2.09E-05	-5.8	-1.2	0.715	ILMN_1231030

Definition

Mus musculus defensin related cryptdin, related sequence 7 (Defcr-rs7), mRNA.

Mus musculus brachyury (T), mRNA.

Mus musculus fibroblast growth factor 17 (Fgf17), mRNA.

PREDICTED: Mus musculus hypothetical protein LOC100044289 (LOC100044289), mRNA.

Mus musculus wingless-related MMTV integration site 3A (Wnt3a), mRNA.

Mus musculus even skipped homeotic gene 1 homolog (Evx1), mRNA.

Mus musculus defensin related cryptdin 6 (Defcr6), mRNA.

Mus musculus fibroblast growth factor 8 (Fgf8), mRNA.

Mus musculus caudal type homeo box 2 (Cdx2), mRNA.

Mus musculus trans-acting transcription factor 5 (Sp5), mRNA.

Mus musculus homeo box C6 (Hoxc6), mRNA.

Mus musculus E26 avian leukemia oncogene 2, 3' domain (Ets2), mRNA.

Mus musculus homeo box A7 (Hoxa7), mRNA.

Mus musculus cyclin-dependent kinase inhibitor 1A (P21) (Cdkn1a), mRNA.

Mus musculus defensin related cryptdin, related sequence 2 (Defcr-rs2), mRNA.

Mus musculus tumor protein D52 (Tpd52), transcript variant 5, mRNA.

Mus musculus CD40 antigen (Cd40), transcript variant 5, mRNA.

Mus musculus HOP homeobox (Hopx), mRNA.

Mus musculus glutamic acid decarboxylase 1 (Gad1), mRNA.

Mus musculus glucosaminyl (N-acetyl) transferase 2, I-branching enzyme (Gcnt2), transcript variant 3, mRNA.

Mus musculus G protein-coupled receptor 83 (Gpr83), mRNA.

Mus musculus LIM domain only 2 (Lmo2), mRNA.

Mus musculus ets variant gene 4 (E1A enhancer binding protein, E1AF) (Etv4), mRNA.

Mus musculus dedicator of cytokinesis 6 (Dock6), mRNA.

Mus musculus transmembrane protease, serine 2 (Tmprss2), mRNA.

Mus musculus interferon regulatory factor 1 (Irf1), mRNA.

Mus musculus sushi domain containing 4 (Susc4), mRNA.

Mus musculus solute carrier family 2 (facilitated glucose transporter), member 3 (Slc2a3), mRNA.

Mus musculus spermine oxidase (Smox), mRNA.

Mus musculus cyclin-dependent kinase inhibitor 1C (P57) (Cdkn1c), mRNA.

Mus musculus UDP-N-acetylglucosamine pyrophosphorylase 1-like 1 (Uap1l1), mRNA. XM_918982

Mus musculus cytochrome P450, family 26, subfamily a, polypeptide 1 (Cyp26a1), mRNA.

Mus musculus glycine decarboxylase (Gldc), mRNA.

Mus musculus pitrilysin metallopeptidase 1 (Pitrm1), mRNA.

Mus musculus acyl-CoA thioesterase 7 (Acot7), mRNA.

Mus musculus scavenger receptor class A, member 3 (Scara3), mRNA.

Mus musculus huntingtin-associated protein 1 (Hap1), mRNA.

Mus musculus wingless-related MMTV integration site 5B (Wnt5b), mRNA.

Mus musculus protein disulfide isomerase associated 5 (Pdia5), mRNA.

Mus musculus endonuclease domain containing 1 (Endod1), mRNA.

Mus musculus nucleoporin 210 (Nup210), mRNA.

Mus musculus defensin related cryptdin 3 (Defcr3), mRNA.

PREDICTED: Mus musculus opioid growth factor receptor-like 1 (Ogfrl1), mRNA.
Mus musculus homeo box C9 (Hoxc9), mRNA.

Mus musculus cysteine rich protein 2 (Crip2), mRNA.
Mus musculus RIKEN cDNA 2610027C15 gene (2610027C15Rik), mRNA.
Mus musculus RAB8B, member RAS oncogene family (Rab8b), mRNA.
Mus musculus slit homolog 2 (Drosophila) (Slit2), mRNA.

Mus musculus homeo box B7 (Hoxb7), mRNA.
Mus musculus microsomal glutathione S-transferase 1 (Mgst1), mRNA.

PREDICTED: Mus musculus similar to Limb expression 1 homolog (chicken) (LOC100045869), mRNA.
Mus musculus sal-like 3 (Drosophila) (Sall3), mRNA.
Mus musculus cDNA sequence AY761185 (AY761185), mRNA.
Mus musculus R-spondin 3 homolog (Xenopus laevis) (Rspo3), mRNA.
Mus musculus sorting nexin 11 (Snx11), mRNA.
Mus musculus furin (paired basic amino acid cleaving enzyme) (Furin), mRNA.
Mus musculus ring finger protein 208 (Rnf208), mRNA.

Mus musculus homeo box C10 (Hoxc10), mRNA.
Mus musculus enolase 3, beta muscle (Eno3), mRNA.
Mus musculus prion protein (Prnp), mRNA.

Mus musculus proline rich region 18 (Prr18), mRNA.
Mus musculus defensin related cryptdin 26 (Defcr26), mRNA.
Mus musculus RIKEN cDNA 2310007H09 gene (2310007H09Rik), mRNA.
Mus musculus WAP four-disulfide core domain 2 (Wfdc2), mRNA.
Mus musculus RIKEN cDNA 1200009O22 gene (1200009O22Rik), mRNA.
Mus musculus nerve growth factor receptor (TNFR superfamily, member 16) (Ngfr), mRNA.
Mus musculus formin binding protein 1 (Fnbp1), transcript variant 1, mRNA.

Mus musculus homeo box D10 (Hoxd10), mRNA.
Mus musculus solute carrier family 1 (glutamate/neutral amino acid transporter), member 4 (Slc1a4), mRNA.
Mus musculus zinc finger, CCHC domain containing 18 (Zcchc18), transcript variant 3, mRNA.
PREDICTED: Mus musculus hypothetical protein LOC100044177 (LOC100044177), mRNA.
Mus musculus serum/glucocorticoid regulated kinase 1 (Sgk1), mRNA.
Mus musculus ornithine aminotransferase (Oat), mRNA.
Mus musculus RIKEN cDNA 1110007M04 gene (1110007M04Rik), mRNA.
Mus musculus ADAMTS-like 2 (Adamtsl2), mRNA.
Mus musculus frizzled homolog 10 (Drosophila) (Fzd10), mRNA.
Mus musculus glutamate receptor, ionotropic, N-methyl D-aspartate-associated protein 1 (glutamate binding) (GluN1), mRNA.
Mus musculus tripartite motif protein 2 (Trim2), mRNA. XM_984114 XM_984144 XM_984172 XM_984200 XM_984230
Mus musculus notum pectinacylesterase homolog (Drosophila) (Notum), mRNA.
Mus musculus CD83 antigen (Cd83), mRNA.

Mus musculus DNA segment, Chr 17, Wayne State University 92, expressed (D17Wsu92e), transcript variant 1, mRNA.
Mus musculus adenomatosis polyposis coli down-regulated 1 (Apcdd1), mRNA.
Mus musculus adrenergic receptor, beta 2 (Adrb2), mRNA.
Mus musculus gamma-aminobutyric acid (GABA(A)) receptor-associated protein-like 1 (Gabarapl1), mRNA.
Mus musculus annexin A3 (Anxa3), mRNA.
Mus musculus zyxin (Zyx), mRNA.

Mus musculus scavenger receptor class A, member 5 (putative) (Scara5), mRNA.

Mus musculus olfactomedin-like 3 (Olfml3), mRNA.

Mus musculus calcium and integrin binding 1 (calmyrin) (Cib1), mRNA.

Mus musculus interleukin 17 receptor D (Il17rd), mRNA.

Mus musculus receptor (calcitonin) activity modifying protein 2 (Ramp2), mRNA.

Mus musculus Notch gene homolog 4 (Drosophila) (Notch4), mRNA.

Mus musculus solute carrier family 1 (glial high affinity glutamate transporter), member 3 (Slc1a3), mRNA.

Mus musculus LY6/PLAUR domain containing 6B (Lypd6b), mRNA.

PREDICTED: Mus musculus sterile alpha motif domain containing 9-like, transcript variant 1 (Samd9l), mRNA.

Mus musculus phosphoglycerate kinase 1 (Pkg1), mRNA.

Mus musculus tropomyosin 1, alpha (Tpm1), mRNA.

PREDICTED: Mus musculus similar to CMP-sialic acid transporter (LOC100046775), mRNA.

Mus musculus E74-like factor 3 (Elf3), mRNA.

Mus musculus centaurin, delta 3 (Centd3), mRNA.

Mus musculus acyl-CoA thioesterase 1 (Acot1), mRNA.

Mus musculus carbohydrate (N-acetylglucosamino) sulfotransferase 7 (Chst7), mRNA.

Mus musculus limb expression 1 homolog (chicken) (Lix1), mRNA.

Mus musculus brain expressed gene 4 (Bex4), mRNA.

Mus musculus BCL2-interacting killer (Bik), mRNA.

Mus musculus cysteine-rich with EGF-like domains 1 (Creld1), mRNA.

Mus musculus hemoglobin X, alpha-like embryonic chain in Hba complex (Hba-x), mRNA.

Mus musculus defensin related cryptdin, related sequence 10 (Defcr-rs10), mRNA.

Mus musculus lymphocyte antigen 6 complex, locus A (Ly6a), mRNA.

Mus musculus secretin (Sct), mRNA.

Mus musculus matrix metalloproteinase 2 (Mmp2), mRNA.

Mus musculus dual specificity phosphatase 6 (Dusp6), mRNA.

Mus musculus ribosomal protein S6 kinase polypeptide 1 (Rps6ka1), mRNA.

Mus musculus forkhead box A3 (Foxa3), mRNA.

Mus musculus gap junction membrane channel protein alpha 1 (Gja1), mRNA.

Mus musculus kelch-like 6 (Drosophila) (Klhl6), mRNA.

Mus musculus LIM and calponin homology domains 1 (Limch1), mRNA.

Mus musculus src homology 2 domain-containing transforming protein C1 (Shc1), mRNA.

Mus musculus myosin light chain, regulatory B (Mylc2b), mRNA.

Mus musculus RAS guanyl releasing protein 4 (Rasgrp4), mRNA.

Mus musculus homeo box D12 (Hoxd12), mRNA.

Mus musculus carbonic anhydrase 14 (Car14), mRNA.

Mus musculus angiopoietin 2 (Angpt2), mRNA.

Mus musculus RELT-like 1 (Rel1), mRNA.

Mus musculus sonic hedgehog (Shh), mRNA.

PREDICTED: Mus musculus similar to Greb1 protein (LOC100045413), misc RNA.

Mus musculus laminin, alpha 1 (Lama1), mRNA.

Mus musculus frizzled homolog 7 (Drosophila) (Fzd7), mRNA.

Mus musculus corticotropin releasing hormone binding protein (Crhbp), mRNA.

Mus musculus thymosin, beta 10 (Tmsb10), mRNA.

Mus musculus leucine rich repeat protein 1, neuronal (Lrrn1), mRNA.

Mus musculus RAS guanyl releasing protein 1 (Rasgrp1), mRNA.

Mus musculus PHD finger protein 17 (Phf17), mRNA.

Mus musculus interferon regulatory factor 6 (Irf6), mRNA.

Mus musculus peptidylprolyl isomerase B (Ppib), mRNA.

Mus musculus RNA binding motif protein 35A (Rbm35a), mRNA.

Mus musculus uridine-cytidine kinase 2 (Uck2), mRNA.

Mus musculus myocardin (Myocd), transcript variant A, mRNA.

Mus musculus paternally expressed 3 (Peg3), mRNA.

Mus musculus DNA-damage-inducible transcript 4-like (Ddit4l), mRNA.

PREDICTED: Mus musculus similar to spermine synthase (LOC671878), mRNA.

Mus musculus myeloid/lymphoid or mixed-lineage leukemia (trithorax homolog, Drosophila); translocated to,

Mus musculus odd Oz/ten-m homolog 4 (Drosophila) (Odz4), mRNA.

Mus musculus chloride intracellular channel 4 (mitochondrial) (Clic4), nuclear gene encoding mitochondrial pi

Mus musculus RIKEN cDNA 1600021P15 gene (1600021P15Rik), mRNA.

Mus musculus calcium/calmodulin-dependent protein kinase II inhibitor 1 (Camk2n1), mRNA.

Mus musculus naked cuticle 2 homolog (Drosophila) (Nkd2), mRNA.

Mus musculus synemin, intermediate filament protein (Synm), transcript variant 3, mRNA.

PREDICTED: Mus musculus zinc finger protein 512B (Znf512b), mRNA.

Mus musculus interferon induced transmembrane protein 1 (Ifitm1), mRNA.

Mus musculus FERM domain containing 6 (Frmd6), mRNA.

Mus musculus tubulin, beta 2b (Tubb2b), mRNA.

Mus musculus procollagen, type V, alpha 1 (Col5a1), mRNA.

Mus musculus sin3 associated polypeptide (Sap30), mRNA.

Mus musculus non-metastatic cells 7, protein expressed in (nucleoside-diphosphate kinase) (Nme7), transcript v

PREDICTED: Mus musculus protocadherin 19 (Pcdh19), mRNA.

Mus musculus phosphoglucomutase 5 (Pgm5), mRNA.

Mus musculus fibroblast growth factor 18 (Fgf18), mRNA.

Mus musculus leucine-rich repeats and immunoglobulin-like domains 1 (Lrig1), mRNA.

Mus musculus Notch-regulated ankyrin repeat protein (Nrarp), mRNA.

Mus musculus interferon induced transmembrane protein 3 (Ifitm3), mRNA.

Mus musculus GDP-mannose 4, 6-dehydratase (Gmds), mRNA.

Mus musculus transcription factor 3 (Tcf3), transcript variant 1, mRNA.

PREDICTED: Mus musculus similar to GFRalpha-3 (LOC100045484), mRNA.

Mus musculus RIKEN cDNA 4631426J05 gene (4631426J05Rik), mRNA.

Mus musculus sPLA/ryanodine receptor domain and SOCS box containing 4 (Spsb4), mRNA.

Mus musculus leucine-rich repeats and immunoglobulin-like domains 3 (Lrig3), mRNA.

Mus musculus PDZ and LIM domain 1 (elfin) (Pdlim1), mRNA.

PREDICTED: Mus musculus similar to phosphoglucomutase 5 (LOC100046963), mRNA.

Mus musculus Notch gene homolog 1 (Drosophila) (Notch1), mRNA.

Mus musculus lipoma HMGIC fusion partner-like 2 (Lhfp12), mRNA.

Mus musculus zinc finger protein 238 (Zfp238), transcript variant 1, mRNA.

Mus musculus transformation related protein 63 (Trp63), mRNA.

Mus musculus pleiotrophin (Ptn), mRNA.
Mus musculus V-set and transmembrane domain containing 2B (Vstm2b), mRNA.
Mus musculus erythrocyte protein band 4.1-like 3 (Epb4.1l3), mRNA.
Mus musculus procollagen, type XVIII, alpha 1 (Col18a1), mRNA.

Mus musculus heparan sulfate (glucosamine) 3-O-sulfotransferase 3A1 (Hs3st3a1), mRNA.
Mus musculus LIM domain only 4 (Lmo4), mRNA.
Mus musculus ripply2 homolog (zebrafish) (Ripply2), mRNA.
Mus musculus keratin 14 (Krt14), mRNA.
Mus musculus Cbp/p300-interacting transactivator, with Glu/Asp-rich carboxy-terminal domain, 2 (Cited2), m
PREDICTED: Mus musculus similar to NFIL3/E4BP4 transcription factor (LOC100046232), mRNA.
Mus musculus forkhead box C2 (Foxc2), mRNA.
Mus musculus reelin (Reln), mRNA.
Mus musculus glutathione peroxidase 2 (Gpx2), mRNA.
Mus musculus ephrin A5 (Efna5), transcript variant 2, mRNA.
Mus musculus solute carrier family 9 (sodium/hydrogen exchanger), member 3 regulator 1 (Slc9a3r1), mRNA.
Mus musculus growth arrest and DNA-damage-inducible 45 gamma (Gadd45g), mRNA.
PREDICTED: Mus musculus RIKEN cDNA 2310047A01 gene (2310047A01Rik), mRNA.
Mus musculus mesoderm posterior 1 (Mesp1), mRNA.
Mus musculus four and a half LIM domains 1 (Fhl1), transcript variant 1, mRNA.
Mus musculus cellular retinoic acid binding protein I (Crabp1), mRNA.

Mus musculus musculin (Msc), mRNA.
Mus musculus forkhead box C1 (Foxc1), mRNA.
Mus musculus sine oculis-related homeobox 1 homolog (Drosophila) (Six1), mRNA.
Mus musculus adducin 3 (gamma) (Add3), mRNA.
Mus musculus SPARC related modular calcium binding 1 (Smoc1), mRNA.
Mus musculus EMI domain containing 2 (Emid2), mRNA.
Mus musculus RAB15, member RAS oncogene family (Rab15), mRNA.
PREDICTED: Mus musculus mastermind like 2 (Drosophila) (Maml2), mRNA.
Mus musculus protein phosphatase 1, regulatory (inhibitor) subunit 1A (Ppp1r1a), mRNA.
PREDICTED: Mus musculus RIKEN cDNA 5430433G21 gene (5430433G21Rik), mRNA.
Mus musculus phosphatidic acid phosphatase type 2B (Ppap2b), mRNA.
Mus musculus Meis homeobox 1 (Meis1), mRNA.
Mus musculus myosin, light polypeptide 1 (Myl1), mRNA.
Mus musculus RIKEN cDNA 2210417D09 gene (2210417D09Rik), mRNA.
Mus musculus fibroblast growth factor receptor 2 (Fgfr2), transcript variant 2, mRNA.
Mus musculus Meis homeobox 2 (Meis2), transcript variant 2, mRNA.
Mus musculus mesenchyme homeobox 1 (Meox1), mRNA.
Mus musculus PDZ domain containing RING finger 3 (Pdzn3), mRNA.

Mus musculus transcription factor 15 (Tcf15), mRNA.

(Grina), mRNA.

1_984238 XM_984275 XM_984313

mRNA. XM_915193 XM_923626 XM_923628 XM_923630 XM_923632

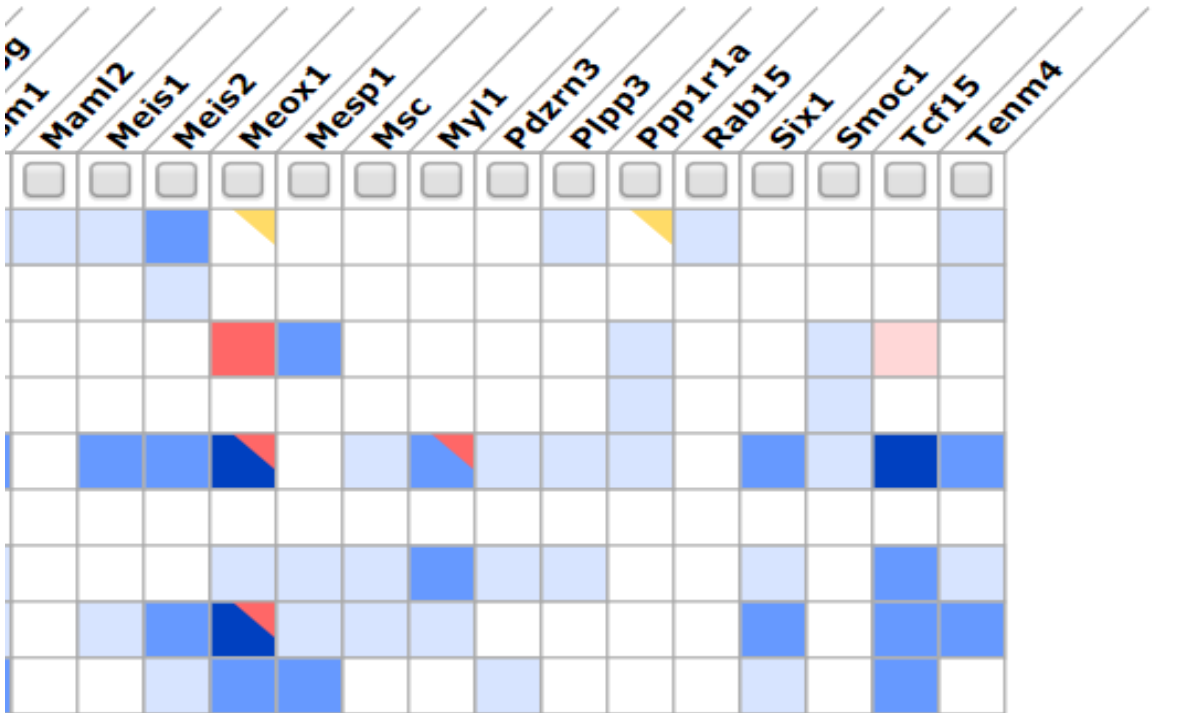
4 (Mllt4), mRNA.

rotein, mRNA.

variant 1, mRNA.

RNA.


Anatomical System Assay Type Detected? Theiler Stage Wild type?
 filters future spinal cord neural plate somite tail paraxial mesenchyme
 primitive streak tail bud
 Chemistry Assay Type: RNA in situ Assay Type: RT-PCR



Gene Expression Database (GXD), Mouse Models of Human Cancer database (MMHCdb) (fc



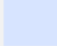
last database update
 06/11/2019
 MGI 6.14

trunk paraxial mesenchyme 




Matrix Legend 

Number of expression results annotated as





present in structure and/or substructures

-  > 50
-  5-50
-  1-4

absent in structure

-  > 20
-  5-20
-  1-4

Other Symbols

-  structure has both present and absent results
-  ambiguous in structure
-  either absent or ambiguous results in substructures
-  no annotations for the gene in this tissue

Filter

Use gray checkboxes to select rows/columns for filtering

[more details](#)

CNH-10.5 (Prapajati et al)	Notochord genes (Wymeier "CNH-10.5" and "Notochord")	Defcr-26	Defcr-rs7	Absc	Olim3	SZ Genes (Pnt Enriched Genes Olvera-Martinez Et, "CNH-10.5" and "SZ")
Defcr26	Defcr26	Defcr-rs7	Ace2	Adams16	Gli2	
Defcr-rs7	Defcr-rs7	Hap1	Adcyap1r1	Agg1	Cyp26a1	
Hap1	Hap1	Hbb-b1	Alcam	Akap12	Evs1	
Hbb-b1	Hbb-b1	Kih16	Ankh	Ankrd50	Fgf8	
Kih16	Kih16	Ndufa4	ApoH	Ap12	Fzd10	
Ndufa4	Ndufa4	Pmp	Arhgap8	Apod	Gja1	
Pmp	Pmp	Scara3	Arhgap17	App1	Greb1	
Scara3	Scara3	Shh	Arl4c	Arid1b	Hoxc9	
Shh	Shh	Shit2	Asf1	Arsb	Il17rd	
Shit2	Shit2		At11	Ast1	Rspo3	
A830080H07RIK	4930533K18RIK		C13orf15	Axin2	Sic1a4	
Acot1	Acot1		C11orf23	Bambi	T	
Acot7	Bicc1		C1orf53	Bbx	Wnt3a	
Adams12	Btg1		C3h2orf43	Bmp2	Wnt5b	
Adrb2	Chrd		C7orf23	Bms1		
Angpt2	Clusterin		C8orf4	Brwd1		
Anxa3	Cob1		C9orf19	C1orf69		
Apod1	Col8a2		C9orf30	C9orf89		
AY761185	Cthrc1		Ca2	Caprin2		
Bex4	Emp1		Cap2	Cbln1		
Bik	Fermt1		Ccap93	Ccdc28a		
C230098021RIK	Ftr3		Cd4	Ccdc82		
Car14	Foxa1		Cited4	Ccdc8a		
Ccnd1	Igfbp5		Ckb	Cd3e		
Cd40	Lmx1a		Cnot6	Cdx2		
Cd63	Ly6H		Coch	Clic4		
Cd83	Moxd1		Col14a1	Cmtm8		
Cd66	Nava3		Ctdsp1	Cmt2		
Cdkn1a	Noto		Dbc1	Comtd1		
Cdkn1c	Nrep		Dhrs3	Crhbp		
Cdx2	Prickle2		Dio2	Csrnp1		
Centd3	Pich1		Ednra	Cwc27		
Chic1	Ppm1		Efemp1	Cyp26a1		
Chst7	scf0003799.1_2		Em1	Cyp27c1		
Cib1	Sema5a		Emi4	Cyt11		
Cpn1	Smoc1		Fabp5	Dach1		
Crelf1	Sox9		Fam5b	Dbf4		
Crip2	Sppl1		Fgf4	Dcbid1		
Cyp26a1	Synpo		Fgf2	Dil1		
D17Wsu92e	Timp3		Fit4	Dock7		
Ddah1			Fn1	Edaradd		
Defcr3			Fzd7	Egr1		
Defcr6			Gcnr7	Enc1		
Defcr-rs10			Gdpp4	Epha1		
Defcr-rs2			Gopc	Epha4		
Dock6			Grm4	Esrig		
Dusp4			Gtf2h4	Etv1		
Dusp6			Gucy1a3	Evs1		
Eif3			Ihna2	F2f1		
Endod1			Itga8	Fabp6		
Eno3			Kcna1	Fam171b		
Ets2			Krt14	Farp1		
Etsrp71			Lgi1	Fgf1		
Etv4			Lmo4	Fgf18		
Ewa1b			Lmx1b	Fgf3		
Evs1			Loc395991	Fgf8		
Fgf17			Loc396300	Fkbp7		
Fgf8			Loc416235	Frdm4b		
Fnbp1			Loc421845	Fzd10		
Foxa3			Loc422305	Ga2		
Furin			Loc769266	Gfa1		
Fzd10			Loc769421	Gja1		
Gabarap1			Lrrm1	Gna11		
Gad1			Ltbp1	Gna13		
Gcnt2			Ly6e	Gnat1		
Gja1			Manea	Greb1		
Gldc			Mapkap1	Hapln1		
Gpr83			Metrnl	Has2		
Greb1			Muc5b	Hoxc9		
Grina			Myk	Hsf5		
Hba-x			Myo3a	Il17rd		
Hoxa			Ndnf	Il1r1		
Hoxa11s			Neurog1	Itga4		
Hoxa7			Nkx6-2	Kat6a		
Hoxb7			Npr3	Kiaa0226i		
Hoxc10			Nr6a1	Le1		
Hoxc6			Olfm1	Lhp12		
Hoxc9			Olfm3	Loc427799		
Hoxd10			Pbx3	Lrig3		
Hoxd12			Pdgfb	Lrrc42		
lap			Pla1a	Lrrc45		
Il17rd			Plek2	Map3k5		
Insr			Plscr4	March6		
Irf1			Ppp2r2a	Mettl6		
Kdm7a			Prdm2	Mid1p1		
Lhpp			Prosl	Mit3		
Lmch1			Prtg	Mpg2		
Lis1			Ptn	Mspg1		
Lmo2			Pts	Mx1		
LOC100044177			Rarb	Mx2		
LOC100044289			Rbm24	Mif2		
LOC100045413			Rcn1	Myc		
LOC100045869			Rffl	Mycf		
LOC100046775			Rfx4	Nefm		
LOC212390			Robo2	Nell2		
Ly6a			Ror1	Nipa1		
Lypd6b			Sdc2	Nop14		
Mgat1			Sdpr	Nsg1		
Mmp2			Sfrp2	Nsun2		
Mylc2b			Shroom1	Nsun3		
Ngfr			Sic398	Ntm		
Notch4			Sic41a2	Pcy11b		
Notum			Sic7a9	Pdcp1		
Nup210			Smad6	Pdc2		
Oat			Snai2	Pde10a		
Ogfr1			Sntb1	Pitpnc1		
Olfm13			Sox18	Rai14		
Pdia5			Sox3	Rasgrp3		
Pgk4			Spag9	Rbm35b		
Pgm2			Sptlc3	Rgs20		
Pitrm1			Sqr1	Rock2		
Prr18			Srs	Rora		
Rab8b			St6galnac2	Rrbp1		
Ramp2			Ston2	Rspo3		
Rasgrp4			Tiam2	S100t		
Rel1			Timp3	Scml2		
Rnf208			Tris2	Sdc3		
Rps6ka1			Ubx4d	Senp5		
Rspo3			Wf1c1	Sic1a4		
Sall3			Zeb2	Sic37a3		
Samd9l				Snal1		
Sbk				Spry2		
Scara5				Srd5a3		
Sct				Suc1p2		
Serpine2				Syndig1		
sgk4				Syp1		
Shc1				Syt10		
Sic1a3				T		
Sic1a4				Thbs4		
Sic2a3				Tmem100		
Simox				Tmem45a		
Snx11				Tnpo1		
Sp5				Tuba4a		
Strbp				Unc5b		
Susd4				Upp1		
T				Uno2		
Tcea3				Vav3		
Thsd2				Wdr66		
Tmprss2				Wnk2		
Tpd52				Wnt3a		
Tpm1				Wnt5a		
Tril				Wnt5b		
Trim2				Xpc		
Uap11				Ythdc1		
Wf1c2				Zeb1		
Wnt3a						
Wnt5b						
Zcchc18						
Zyx						

Enrichment analysis report													
Enrichment by Pathway Maps													
#	Maps	Total	min(pValue)	Min FDR	(1) CNH Vs. PSM.diffGenes.up				(2) CNH Vs. PSM.diffGenes.dn				
					p-value	FDR	In Data	Genes from Active Data	p-value	FDR	In Data	Genes from Active Data	
1	Development Notch Signaling Pathway	43	7.829E-09	8.3766E-07	2.594E-01	3.707E-01	1	Furin	7.829E-09	8.377E-07	6	p63, NOTCH1 (NICD), SAP30, NOTCH1 (NEXT), NOTCH1 precursor, NOTCH1 receptor	
2	Transcription Androgen Receptor nuclear signaling	45	5.702E-07	0.00014996	5.702E-07	1.500E-04	6	p21, Frizzled, Shc, M	1.520E-01	2.544E-01	1	Frizzled	
3	Development NOTCH-induced EMT	19	4.095E-05	0.00146043	1.241E-01	3.707E-01	1	NOTCH4	4.095E-05	1.460E-03	3	NOTCH1 (NICD), NOTCH1 (NEXT), NOTCH1 receptor	
4	Development Regulation of epithelial-to-mesenchymal transition (EMT)	64	7.567E-05	0.00767064	7.567E-05	7.671E-03	5	NOTCH4, Frizzled, M	2.256E-02	2.195E-01	2	Frizzled, NOTCH1 receptor	
5	Cytoskeleton remodeling TGF_WNT and cytoskeletal remodeling	111	1.113E-04	0.00767064	1.113E-04	7.671E-03	6	MRLC, p21, Frizzled,	7.472E-03	1.148E-01	3	MELC, Frizzled, Tcf(Lef)	
6	Development MAG-dependent inhibition of neurite outgrowth	37	1.167E-04	0.00767064	1.167E-04	7.671E-03	4	MRLC, NGFR (ICD), N	1.267E-01	2.544E-01	1	MELC	
7	Translation Non-genomic (rapid) action of Androgen Receptor	40	2.617E-03	0.07647765	2.617E-03	7.648E-02	3	Frizzled, Shc, WNT	1.363E-01	2.544E-01	1	Frizzled	
8	Development Melanocyte development and pigmentation	49	4.670E-03	0.08058998	4.670E-03	8.059E-02	3	p90RSK1, Frizzled, W	1.644E-01	2.544E-01	1	Frizzled	
9	Cytoskeleton remodeling Cytoskeleton remodeling	102	5.371E-03	0.08058998	5.371E-03	8.059E-02	4	MRLC, p21, Shc, Zyx	5.295E-02	2.544E-01	2	MELC, Tcf(Lef)	
10	Development WNT signaling pathway Part 2	53	5.822E-03	0.08058998	5.822E-03	8.059E-02	3	Frizzled, WNT, Cyclin	1.581E-02	1.692E-01	2	Frizzled, Tcf(Lef)	

Table S5. List of primers sequences

Primer name	Sequences (5' to 3')
mGreb1 For	GCCACGGGGCGTCCGGCCCTTTC
mGreb1 Rev	ACCGCGCTGTGCAGGCGGGGGA
chGreb1-For	ATCCGCAAGGGGAGTCTTTACC-3
chGreb1-Rev	GGTGAGGAGGATGAGGAGGTGA
zGreb1-For	AAGGAGCCACCCCTCTGCACATTCT
zGreb1-Rev	TTAGACGAAACCGCATTTCGTCCTC
M1-RT-PCR-for	GGAGTCTGACCGCCAGTGACCAG
M1-RT-PCR-rev	AAGTGCATTACGTCCACATTCATCG
M2-RT-PCR-for	GCTTGTCTCTGAAGGAGGCTGAGCA
M2-RT-PCR-rev	ATTCTCCCTGTGGATCCATGCCAGT